The Modeling of Structure and Properties of Carburized Low-Chromium Hypereutectoid Steels

M. Przylecka

Research of carburized high-carbon bearing LH15 (52100) steel is presented. Problems analyzed include thermodynamic and kinetic basis of carburizing in two-phase field (austenite-cementite), carbon content influence in diffusive layer on utilization properties of the examined steel, and functional carbon content influence on chemical and phase composition of carbonized layer. An understanding of these problems enables modeling of functional properties and chemical and phase composition diffusion layers, obtained at definite carburizing parameters. That is the choice of carburizing process parameters (temperature, time, carbon potential) for the best utilizable properties.

Keywords
bearing steel, carburize modeling, carburizing

1. Introduction

MANY authors were interested in increasing the life of bearing elements made from LH15 steel (52100 grade steel according to ASTM-A295-70) by modifying its chemical composition. The bearing steel carburizing process and its influence on utilizable properties was also a subject of the investigations.

The carburized layer formed on machine elements made of hypereutectoid low-chromium LH15 (52100) steel increases considerably their functional properties. Its presence increases resistance of these elements to frictional wear and fatigue, increases hardness, and decreases friction coefficient (Ref 1). The best functional properties of the layer are connected with appearance in its surface zone of 1.8 to 2.0% C. This paper presents the influence of carburizing parameters and heat treatment after carburizing on limited volumetric fatigue strength, hardness, contact fatigue life, abrasive wear intensity, martensitic transformation start temperature, and phase analysis of diffusion layers formed on LH15 steel. The influence of the type of carburizing atmosphere, temperature, and time on carbon concentration changes when two-phase structure is defined.

The problems encountered when carburizing low-carbon steels were completely presented in Ref 2. The influence of chemical and phase composition on utilizable properties of hypereutectoid bearing steels was extensively presented in Ref 1 and 3. Reference 7 presents the model of chemical and phase composition calculations for carburized layers formed on LH15 (52100) steel. The Parrish correction for two-phase fields (austenite-cementite) was determined in Ref 7. The model of calculations described in Ref 7 was used to predict chemical and phase composition for carburized layers formed on LH15 (52100) steel. References 4 through 6 present thermodynamic and kinetic analysis of the carburizing process in two-phase fields (austenite-cementite) at 1173 K. Carbon activity in two-phase fields of the Fe-Cr-C and Fe-Cr-Mn-Si-C alloys is given by new experimental equations as a function of C content in alloy and C potential of atmosphere (Ref 4). This relation makes possible controlled carburizing of LH15 grade bearing steel. The influence of C potential and carburizing time on the C profile in LH15 (52100) bearing steel at 1173 K was described in detail in Ref 5. From the investigations, the highest utilizable properties can be obtained for 1.8 to 2.0% C in the layer of the upper zone. For higher contents, utilizable properties decrease diffusion layers formed on LH15 steel.

M. Przylecka, Poznań University of Technology, Institute of Mechanical Technology, Heat Treatment Division, ul.Piotrowo 3, 61-138 Poznań, Poland.

2. Thermodynamic and Kinetic Model of Controlled Carburizing Process in Two-Phase Fields Austenite-Cementite

2.1 *Carbon Activity in Two-Phase Fields of the Fe-Cr-Mn-Si-C Alloys at 1173 K*

The effects of various alloying elements on C activity in austenite have been studied by many investigators. The influence of chromium, manganese, and silicon, on C activity in alloyed austenite was presented in Ref 8 and 9. These observations included a number of compositions in the two-phase fields, γ + carbides. The effect of Cr on C activity in the two-phase fields at 1273 and 1373 K was accurately studied in Ref 10 and 11.

Carbon activity in the Fe-Cr-C, Fe-Mn-C, and Fe-Si-C alloys was studied (Ref 4) by equilibration with controlled carburizing atmospheres at 1173 K. Research shows that C activity is diminished by Cr and Mn and increased by Si. The results in the austenite field agree with Ref 8 and 9. In two-phase fields of the Fe-Cr-C and Fe-Cr-Mn-Si-C alloys, C activity is given by new experimental equations according to C content in alloy and C potential of atmosphere. This relation enables controlled carburizing of LH15 (52100) grade bearing steel.

2.1.1 Experimental Procedure

Carbon activity of the Fe-Cr-C, Fe-Mn-C, and Fe-Si-C alloys was studied by equilibration with controlled carburizing atmospheres at 1173 K and to about 1.55% Cr, 1.7% Mn, and 1.53% Si (Ref 4). The atmosphere of fixed compositions (cracked methanol with propane-butane gas or with ethyl acetate) was used. This gas mixture does not protect against internal oxidation, but C transfer coefficient and secondary C

availability of this atmosphere obtain high values. Arrangements are shown in Fig. 1. Specimens were shaped in foils of about 60 by 10 by 0.05 mm. Two specimens—pure iron and Fe-Cr, Fe-Mn, or Fe-Si alloy—were put into the quartz tube and were carburized to obtain equilibrium with atmosphere. The final C content of specimens was determined by chemical analysis. Carbon content in pure Fe-C alloys corresponds to C potential of atmosphere.

2.1.2 Results and Discussion

Figure 2 shows the influence of C potential (C content in pure Fe-C alloy) on the C content in Fe-Cr-C, Fe-Mn-C, or Fe-Si-C specimens in equilibrium with carburizing atmosphere. Experimental results agree with Eq 1 to 3 (Ref 4).

For Fe-Cr-C alloys, carbon content (wt%) is:

$$C_{FeCr} = C_{Fe}\left(1 + \frac{Cr}{10} + \left\{1 - \exp\left[-(C_{Fe} - A)^{10}\right]\right\}\right) \quad \text{(Eq 1)}$$

For Fe-Mn-C alloys, carbon content (wt%) is:

$$C_{FeMn} = C_{Fe}\left(1 + \frac{Mn}{3.03}\right) \quad \text{(Eq 2)}$$

For Fe-Si-C alloys, carbon content (wt%) is:

$$C_{FeSi} = C_{Fe}\left(1 - \frac{Si}{8.38}\right) \quad \text{(Eq 3)}$$

where C_{Fe} is carbon potential (carbon content in pure Fe-C alloy) and A, an experimental value, is dependent on Cr content; that is, $A = 2.4942 \exp(-1.6874\ Cr)$.

These expressions are compared with results of Ref 12 to 14, in which alloying factors were given by equations (for austenite of the Fe-Cr-Mn-Si-C alloys).

According to Sauer et al. (Ref 12):

$$\log \frac{C_{Fe}}{C_{FeCrMnSi}} = -0.04\%\ Cr - 0.01\%\ Mn + 0.075\%\ Si \quad \text{(Eq 4)}$$

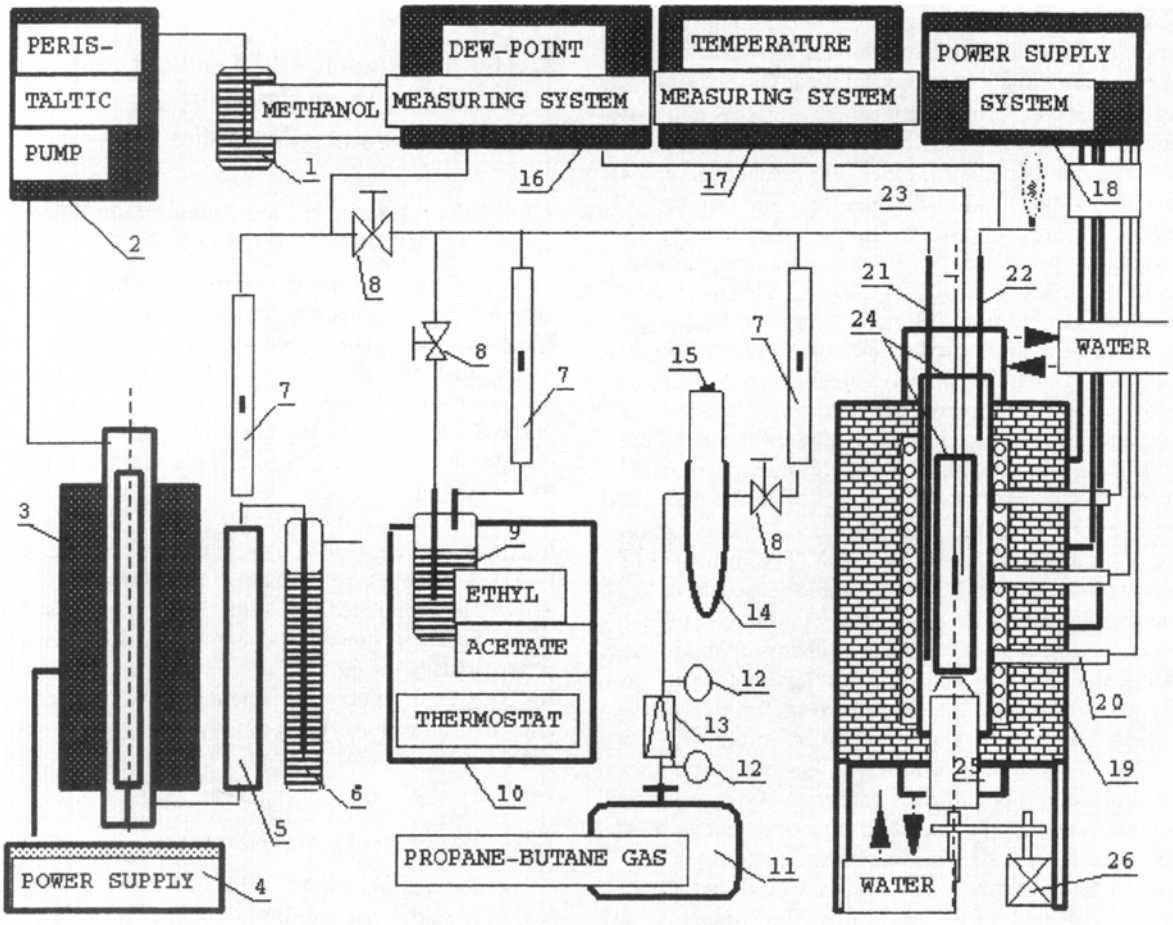

Fig. 1 Arrangements used by experiments. 1, methanol; 2, perstaltic miniflow pump; 3, generator of atmosphere; 4, power supply system; 5, water cooler; 6, manostat; 7, rotameter; 8, valve; 9, ethyl acetate; 10, thermostat; 11, propane-butane gas; 12, manometer; 13, pressure-reducing valve; 14, U-tube manometer; 15, ruff; 16, dew-point measuring system; 17, temperature measuring system; 18, electronic power supply system; 19, carburizing furnace; 20, regulating thermoelement; 21, gas input; 22, gas output; 23, measuring thermoelement; 24, internal and external quartz tubes; 25, ventilator; 26, motor of ventilator

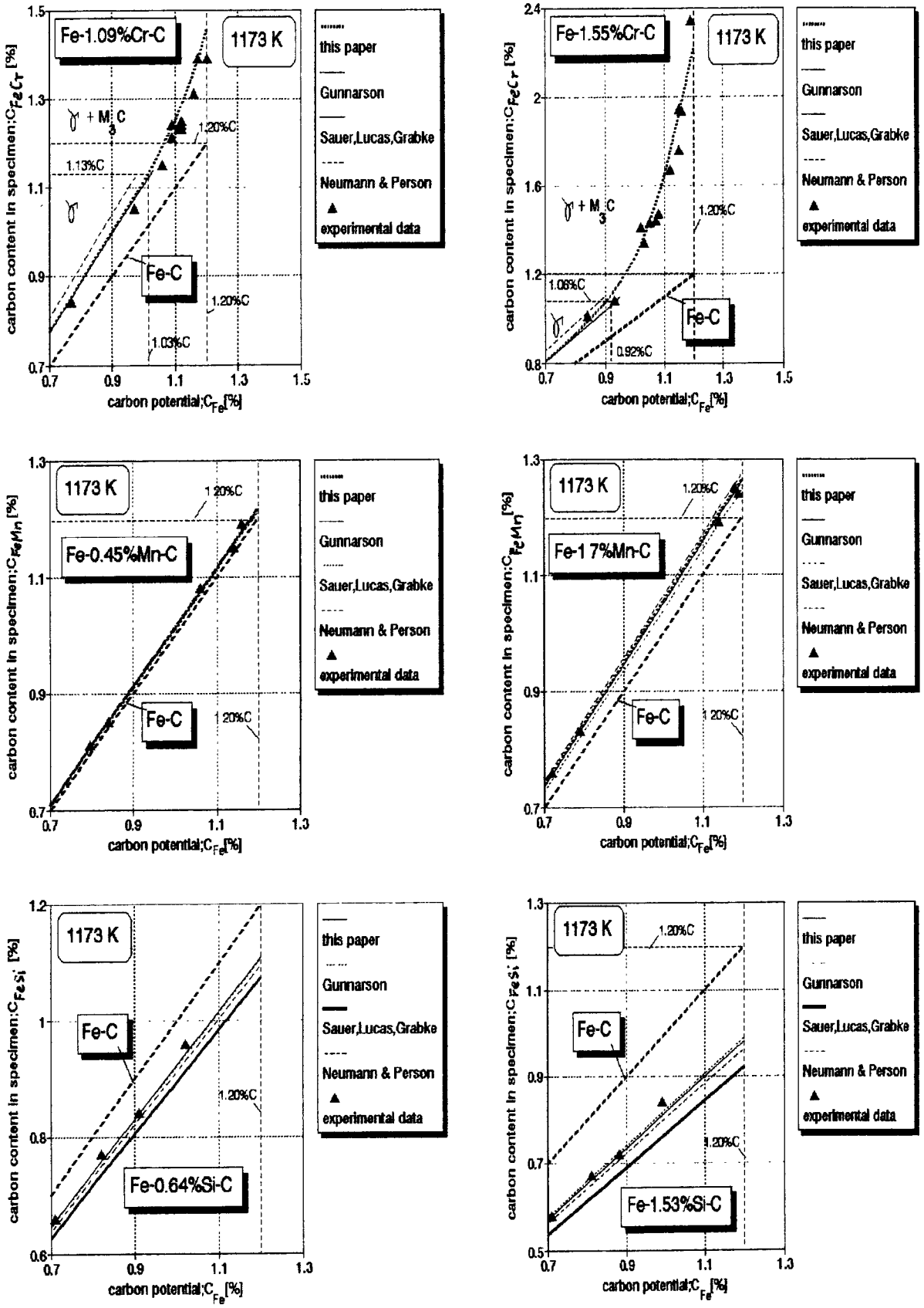

Fig. 2 Influence of carbon potential on the carbon content of Fe-Cr-C, Fe-Mn-C, and Fe-Si-C specimens in equilibrium with carburizing atmosphere at 1173 K (Ref 4)

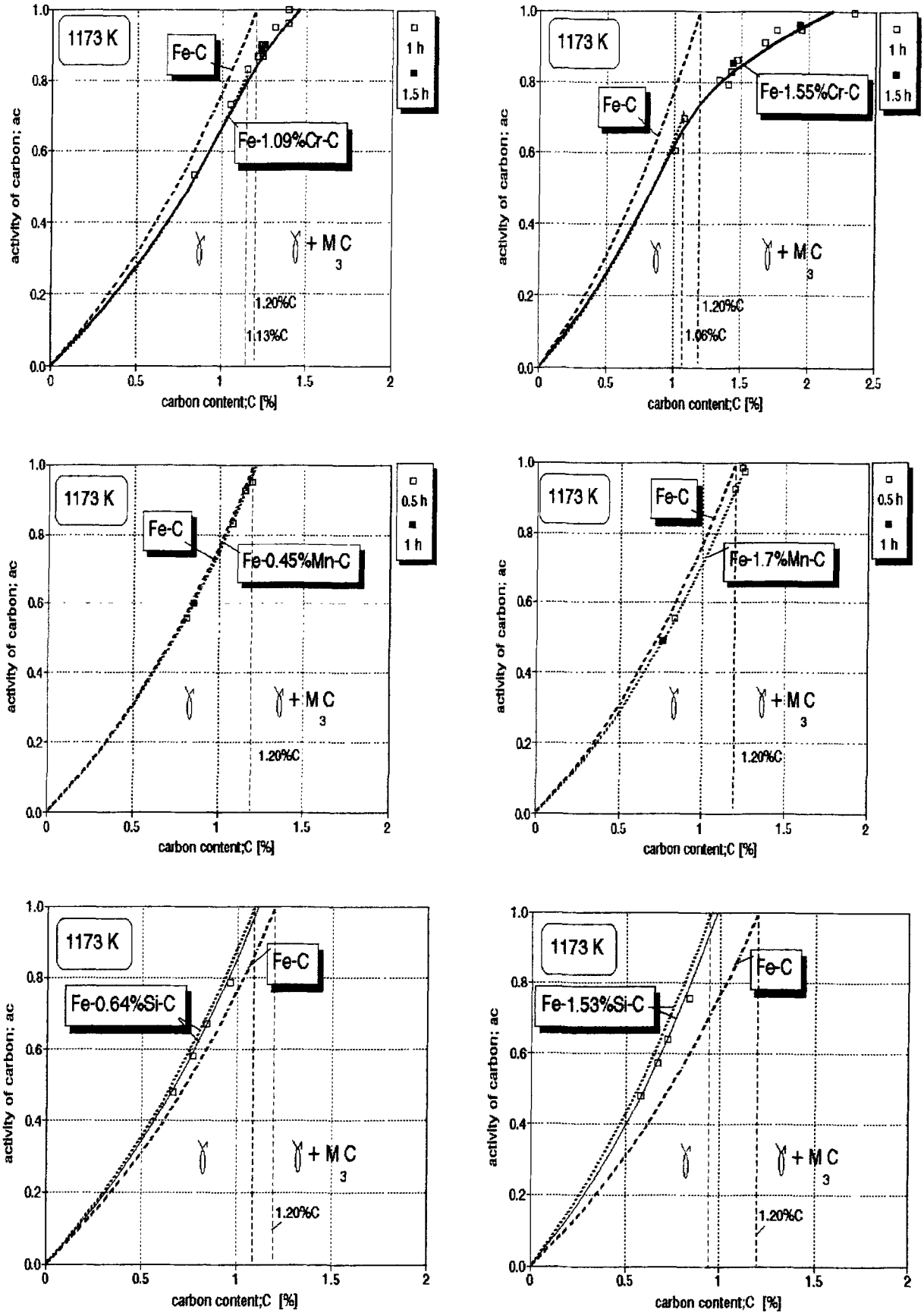

Fig. 3 Activity of carbon in the Fe-Cr-C, Fe-Mn-C, and Fe-Si-C alloys in relation to the carbon content at 1173 K (Ref 4)

According to Neumann and Person (Ref 13):

$$\log \frac{C_{Fe}}{C_{FeCrMnSi}} = -0.057\%\ Cr - 0.016\%\ Mn + 0.062\%\ Si \quad \text{(Eq 5)}$$

According to Gunnarson (Ref 14):

$$\log \frac{C_{Fe}}{C_{FeCrMnSi}} = 0.04\%\ Cr - 0.013\%\ Mn + 0.055\%\ Si \quad \text{(Eq 6)}$$

Carbon activity was calculated (Ref 15) from the C content of the pure Fe specimen using Eq 7.

$$\log a_C = \frac{2300}{T} - 0.92 + \frac{3860}{T} Y_C + \log Z_C \quad \text{(Eq 7)}$$

where

$$Y_C = \frac{n_C}{n_{Fe}}$$

$$Z_C = \frac{n_C}{n_{Fe} - n_C}$$

n_C and n_{Fe} are the number of atoms of C and Fe, respectively, in an alloy, and T is temperature in kelvin.

Figure 3 presents experimental results of C activity in function of C content in the alloys used. These results (for Fe-Cr-C and Fe-Mn-C alloys) agree with data of Ref 8 and 9 for austenite. The biggest influence of the internal oxidation was observed in Fe-Si-C alloys.

Based on Eq 1 to 3, the C content in Fe-Cr-Mn-Si-C alloy in equilibrium with carburizing atmosphere is (Ref 4):

$$C_{FeCrMnSi} = C_{Fe}\left\{1 + \frac{Cr}{10} + \frac{Mn}{30.3} - \frac{Si}{8.38} + 1 - \exp[-(C_{Fe} - A)^{10}]\right\} \quad \text{(Eq 8)}$$

Equation 8 may be used for austenite and for two-phase fields (austenite-cementite). This expression was used to calculate the C activity of the Fe-Cr-Mn-Si-C alloys and to determine the maximal C content at the carburized layer surface on LH15 (52100) steel. Increasing carburizing time increases C content at the surface until equilibrium with carburizing atmosphere is obtained.

2.2 *Influence of Carburizing Parameters on the Carbon Profile in LH15 (52100) Steel at 1173 K*

In Ref 5, the influence of C potential and carburizing time on the C profile in LH15 (52100) bearing steel at 1173 K was presented. The results of C profile research in a carburized layer formed on LH15 steel agree with maximal C content at the surface calculated with Eq 8 (Ref 4, 6). The influence of C potential of the atmosphere and carburizing time on the C concentration at the surface was determined. The C concentration at the surface obtained by C potential 1.2% C corresponds to the best functional properties of carburized LH15 steel. The new experimental equations for two-phase fields (austenite-cementite) were determined (Ref 5, 6). These equations describe the influence of the carburizing parameters (C potential and carburizing time) on the C profile (the C content in function of distance from the surface) in carburized LH15 (52100) steel at 1173 K.

2.2.1 Experimental Procedure

The carburized layers in LH15 (52100) steel were formed by controlled carburizing atmospheres at 1173 K (Ref 5). The arrangements are shown and described in Fig. 1. The atmosphere of a fixed composition (cracked methanol with propane-butane gas or with ethyl acetate) was used. Specimens were shaped in rollers about 15 mm diameter and 100 mm long. Then they were put into the quartz tube and were carburized at fixed C potentials and fixed times. Three fixed C potentials (1.1, 1.2, and 1.48% C) and three fixed times of carburizing (2, 5, and 15 h) were used. Carbon contents were determined by chemical analysis of successive layers. Carbon potential was controlled by the dew-point measuring system and by pure Fe-C foils carburized until equilibrium with atmosphere was obtained. Carbon content in pure Fe-C alloy corresponds to C potential of atmosphere. Table 1 presents the chemical composition of LH15 steel.

Carbon potentials used by experiments were determined in wt% (Ref 4, 6) using Eq 9.

$$C_{FeCrMnSi} = C_{Fe}\left\{1 + \frac{Cr}{10} + \frac{Mn}{30.3} - \frac{Si}{8.38} + 1 - \exp[-(C_{Fe} - A)^{10}]\right\} \quad \text{(Eq 9)}$$

where C_{Fe} is carbon potential (C content in pure Fe-C alloy); $C_{FeCrMnSi} = C_{max}$ is carbon content in Fe-Cr-Mn-Si-C alloy; and A, an experimental value, is dependent on Cr content; that is, $A = 2.4942 \exp(-1.6874\ Cr)$.

Table 1 Chemical composition of LH15 (52100) steel

Element	Composition, wt %
C	1.00
Cr	1.44
Mn	0.31
Si	0.21
P	0.019
S	0.020
Ni	0.16
Cu	0.12
V	0.005
Mo	0.029
W	0.006
Ti	0.002
Co	0.007
Al	0.065
B	0.0004

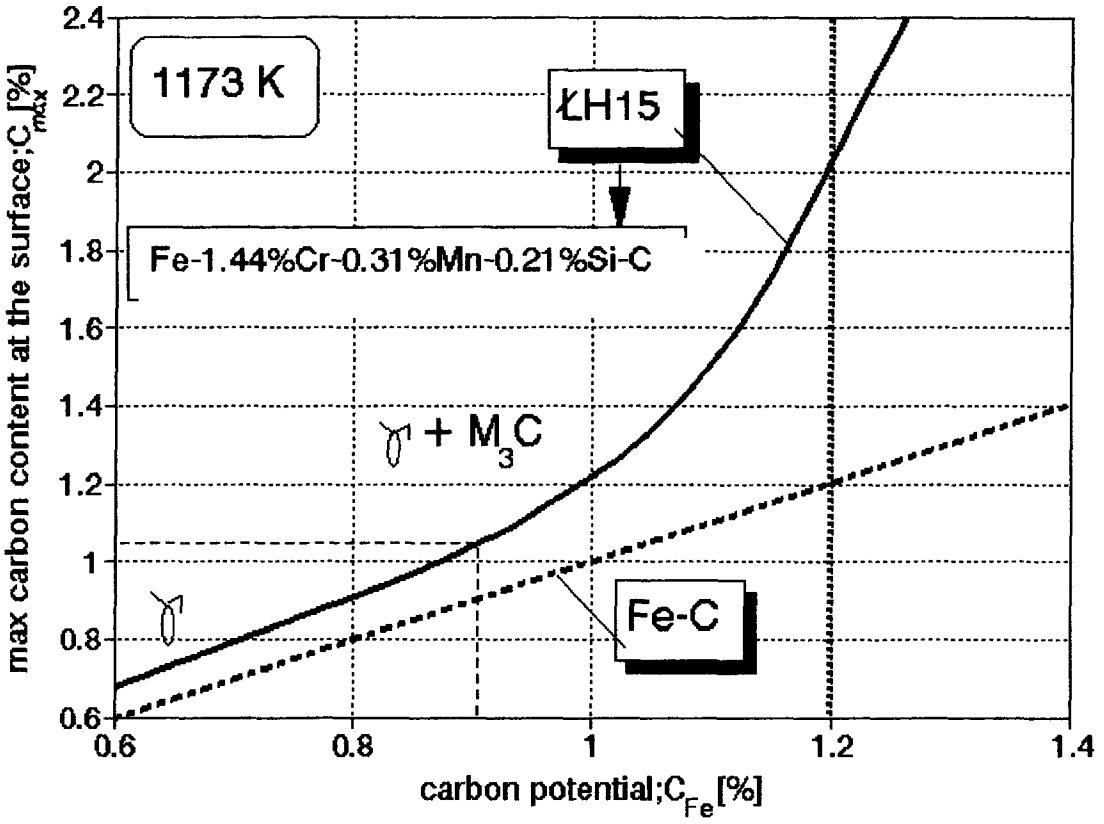

Fig. 4 Influence of carbon potential on the maximal carbon content at the surface in carburized LH15 (52100) steel at 1173 K (Ref 4, 6)

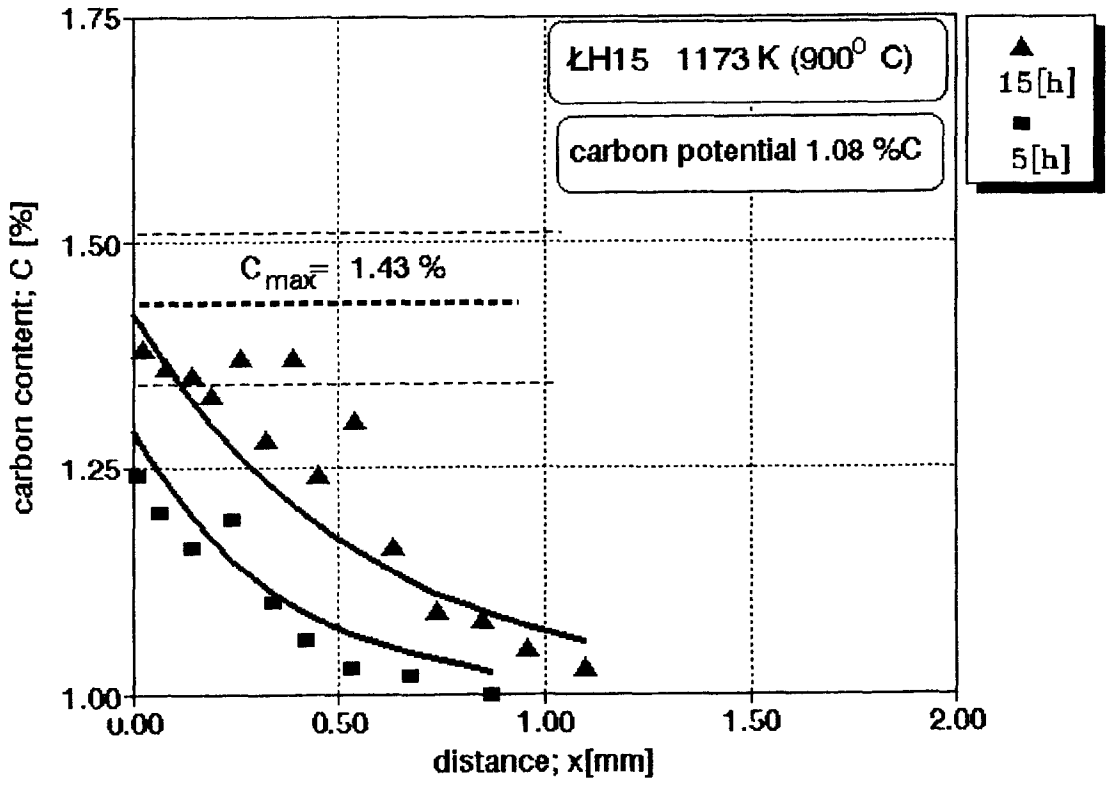

Fig. 5 Carbon profiles of carburized layer formed on LH15 (52100) steel at 1173 K (fixed carburizing times) (Ref 5)

This expression describes the influence of C potential (C_{Fe}) on the C content in Fe-Cr-Mn-Si-C alloy in equilibrium with carburizing atmosphere at 1173 K. Equation 9 was used to calculate the C activity of Fe-Cr-Mn-Si-C alloys and to determine the maximal surface C content in carburized layer formed on LH15 (52100) steel. Figure 4 presents the results of calculations. The chemical composition of LH15 steel, presented in Table 1, was used in these calculations.

2.2.2 Results and Discussion

Figures 5 to 7 show the influence of carburizing times on the C profile in LH15 steel at given C potentials at 1173 K (Ref 5). Figures 5 to 7 show that increase of carburizing time is accompanied by increase of C content at the surface until equilibrium with carburizing atmosphere is obtained. The maximal C content at the surface was calculated with Eq 9. The highest C concentration at the surface obtained by all C potentials involved corresponds to maximal C content calculated using Eq 9. In Fig. 5 to 7, dashed lines show the influence of C potential changes on the maximal C content at the surface.

Experimental C profiles of a carburized layer on LH15 steel agree with those obtained using Eq 10 (Ref 5).

$$C_x = C_o + (C_s - C_o) \exp(-Dx) \quad \text{(Eq 10)}$$

where C_x is carbon content (wt%) in carburized layer of LH15 steel in the x-distance from the surface; C_o is carbon content (wt%) in LH15 steel at the start of carburizing; C_s is carbon content (wt%) at the surface, which is dependent on carbon potential and carburizing time; x is distance (mm) from the surface; and D is a coefficient that is dependent on carbon potential and carburizing time.

Figure 8 shows the influence of C potential of the atmosphere, C_{Fe}, and carburizing time on the surface C concentration, C_s. The increase of C potential and carburizing time is accompanied by an increase of surface C content. The experimental results agree with the curves described using Eq 11 (Ref 5):

$$C_s = C_{max} - (C_{max} - C_o) \exp(-Bt) \quad \text{(Eq 11)}$$

where C_o is carbon content (wt%) in LH15 steel at the start of carburizing; $C_{max} = C_{FeCrMnSi}$ is maximal carbon content at the surface calculated using Eq 9; t is carburizing time (h); and B is a coefficient that is expressed as $B = 0.5452 (C_{max} - C_o)$.

The D coefficient in Eq 10 may be expressed as (Ref 5):

$$D = \frac{1}{t^c}\left[a\left\{1 - \exp[-b(C_{Fe} - C^o_{Fe})]\right\} + d(C_{Fe} - C^o_{Fe}) \exp(-et)\right] \quad \text{(Eq 12)}$$

where t is carburizing time (h); C_{Fe} is carbon potential (wt%) of atmosphere (carbon content in pure Fe-C alloys); C^o_{Fe} is carbon potential (wt%) of atmosphere in equilibrium with LH15 steel at the start of carburizing; and a, b, c, d, and e are experimental values. This equation agrees with experimental results of C profiles of the layers on LH15 steel. Figure 9 shows the influence of carburizing time and C potential on the D coefficient value.

2.3 *Conclusions*

Calculations of the C activity of the Fe-Cr-Mn-Si-C alloys in austenite and in two-phase fields at 1173 K were determined in Ref 4 and Eq 8. This expression was used to determine the maximal C content at the surface in the carburized layer formed on hypereutectoid low-chromium LH15 (52100) steel after controlled carburizing. The results of C profile research in the carburized layer on LH15 steel agree with maximal C content at the surface calculated by this equation. In Ref 5, the new experimental equations for two-phase fields (austenite-cementite) were determined. Equation 10 describes the C profile (C content as a function of distance from the surface) in carburized LH15 steel. Equation 11 presents the influence of C potential and carburizing time on the C content at the surface in LH15 steel. Equation 12 describes the D coefficient value from Eq 10 as a function of carburizing time and C potential of atmosphere. Carbon concentration at the surface obtained by the carbon potential 1.2% C at 1173 K corresponds to the best functional properties of carburized LH15 steel.

3. Influence of Carbon Content in the Carburized Layer on the Functional Properties of Low-Chromium Hypereutectoid Steels

The carburized layer formed on machine elements made of low-chromium hypereutectoid LH15 (52100) steel increases considerably their functional properties. Its presence increases resistance of these elements to frictional wear and fatigue, increases hardness, and decreases the friction coefficient (Ref 1). The best functional properties of the layer are connected with appearance in its surface zone of C content ranging from 1.8 to 2.0% C. This investigation presents results of the influence of fixed factors (carburizing parameters, heat treatment after carburizing, and C content at the surface) on limited volumetric fatigue strength, hardness, contact fatigue life, and abrasive wear intensity of diffusion layers formed on LH15 steel. The relevant study was used.

3.1 *Experimental Procedure*

Investigation results are related to chemical composition of used LH15 bearing steel, according to PN-74/H-84041 (Table 2). The parameters of carburizing and heat treatment are listed in Table 3. The carburized layers in LH15 (52100) steel were formed by controlled carburizing atmospheres at 1173 K.

Table 2 Chemical composition of 20H and LH15 steels used by experiments

Material	Composition, wt%					
	C	Cr	Mn	Si	Ni	Cu
20H	0.20	0.94	0.61	0.27	0.13	0.17
LH15 (52100)	1.00	1.43	0.24	0.29	0.04	0.20

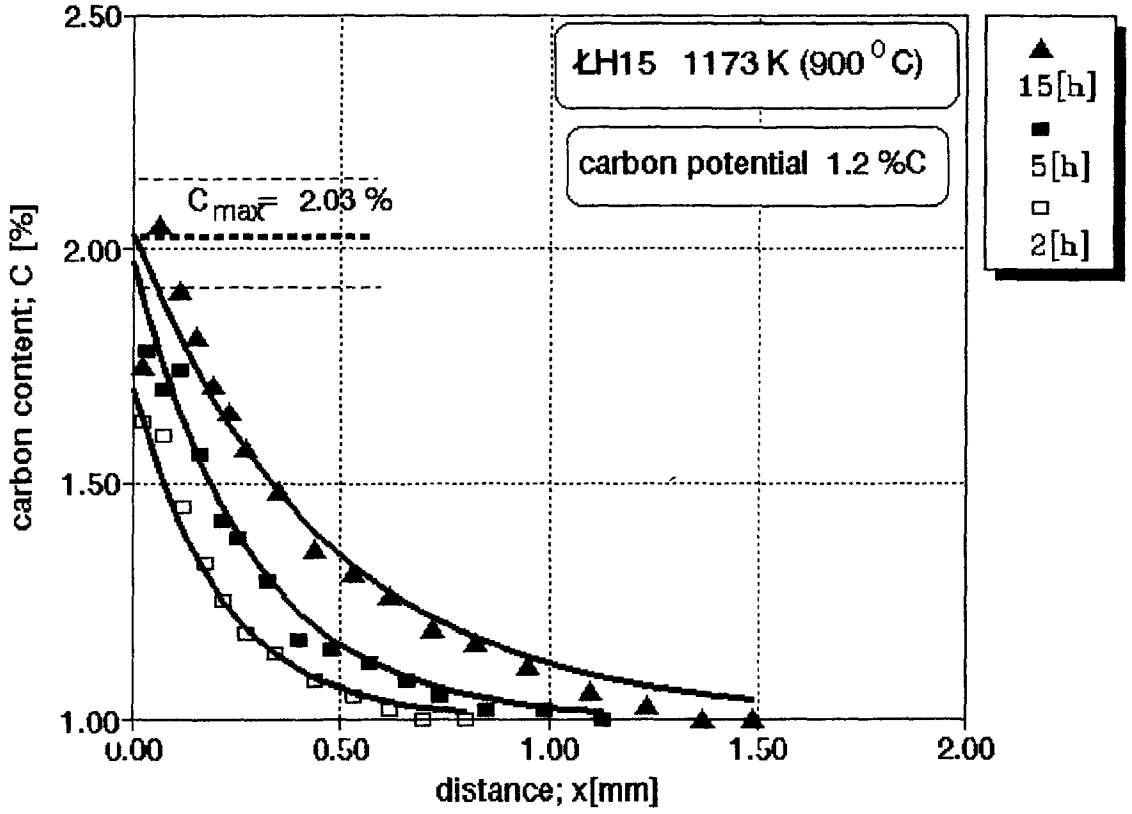

Fig. 6 Carbon profiles of carburized layer formed on LH15 (52100) steel at 1173 K (fixed carburizing times) (Ref 5)

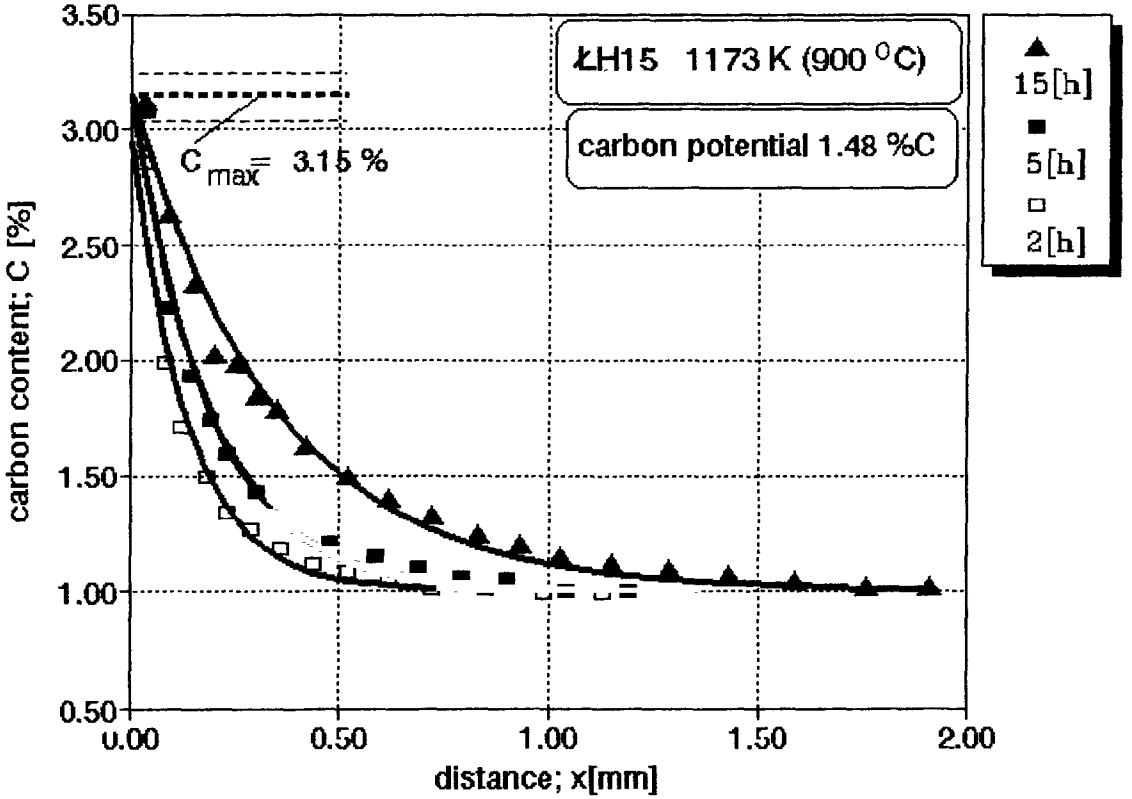

Fig. 7 Carbon profiles of carburized layer formed on LH15 (52100) steel at 1173 K (fixed carburizing times) (Ref 5)

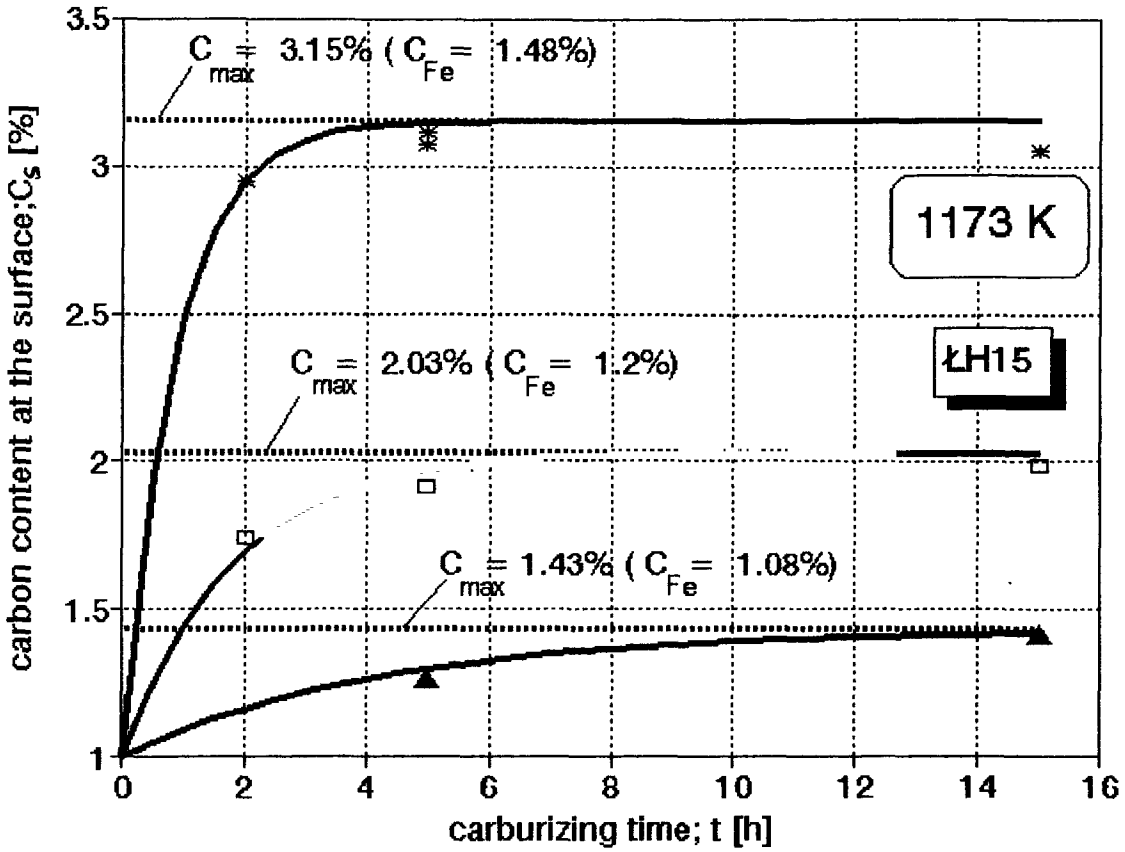

Fig. 8 Influence of carburizing time and carbon potential C_{Fe} on the carbon content at the surface of carburized LH15 (52100) steel at 1173 K (Ref 5)

Table 3 Variants of heat treatment after carburizing

	Carburizing		Hardening						Tempering	
			Austenitizing		Cooling		After cooling			
Variant	Temperature (T_n), K	Time (t_n), h	Temperature (T_a), K	Time (t_a), h	Temperature (T_{ch}), K	Time (t_{ch}), h	Temperature (T_d), K	Time (t_d), h	Temperature (T_o), K	Time (t_o), h
1	1173	15	1123	0.3	393 oil	0.1	283 water	0.5	453	2
2	1173	15	1123	0.25	393 oil	0.1	283 water	0.2	423	1
3	1173	15	1073	0.25	393 oil	0.1	283 water	0.2	423	1
4	1173	15	1123	0.25	293 oil	0.3	...	...	423	1
5	1173	15	1073	0.25	293 oil	0.3	...	...	423	1
6	1173	15	1123	0.25	293 water	0.3	...	...	423	1
7	1173	15	1073	0.25	293 water	0.3	...	...	423	1
8	...	...	1123	0.3	393 oil	0.1	283 water	0.5	453	2

The atmosphere of fixed composition (cracked methanol with propane-butane gas or with ethyl acetate) was used. Figures 5 to 7 present the dependence of the total C content variations upon the distance from surface of carburized bearing steel. The C contents were determined by chemical analysis of successive layers.

Based on Fig. 5 to 7, the samples were ground to obtain a different surface total C content. Samples prepared in this manner were heat treated according to parameters selected in Table 3. Fatigue strength tests were carried out according to PN-76/H-04326, and hardness tests (Rockwell and Vickers methods) were according to PN-78/H-04355 and PN-78/H-04360, respectively (Ref 16, 17). Experimental procedures of contact fatigue life and abrasive wear intensity were presented in Ref 1. The influence of C content in the two-phase fields (LH15 and 20H steels) on the bending strength, tensile strength, and impact strength was studied (Ref 19). The same samples were used to determine a longitudinal modulus of elasticity (Young's modulus).

3.2 *Investigation Results*

Figure 10 shows that maximal fatigue strength is obtained for 1.6 to 1.9% of the total surface C content of the sample. It

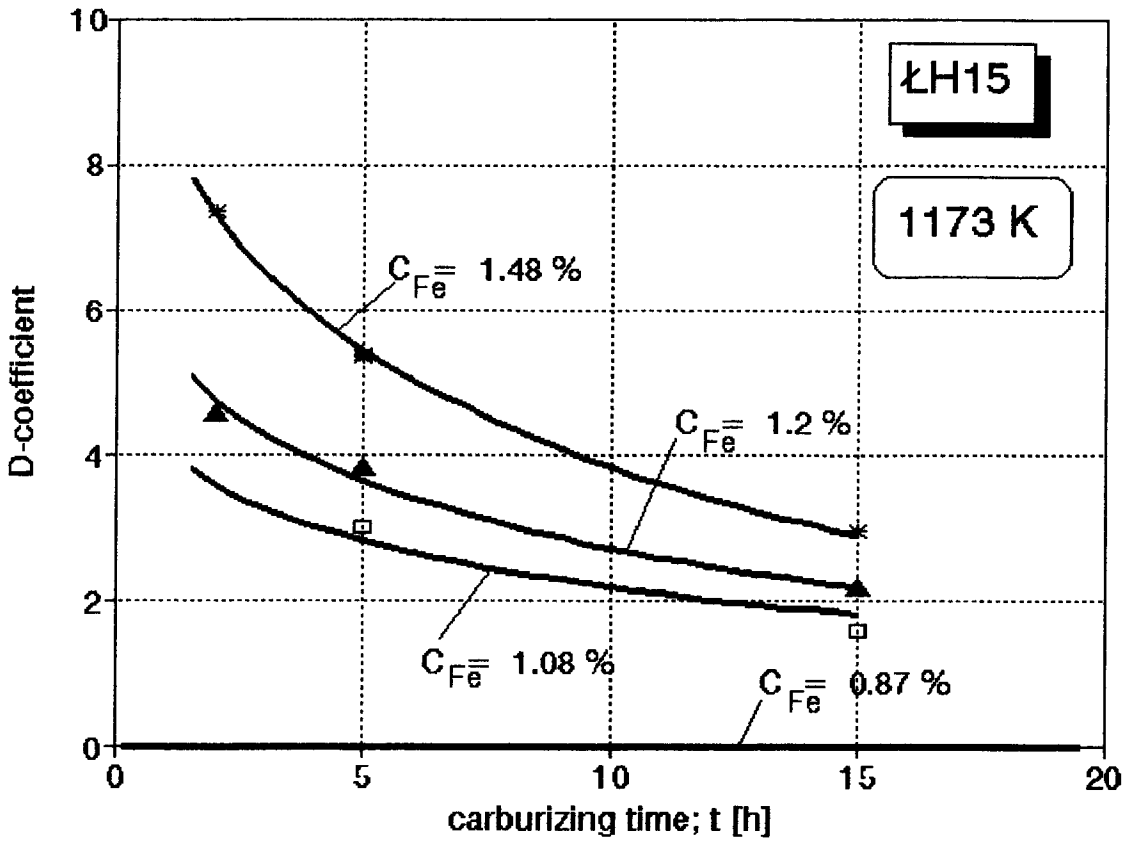

Fig. 9 Influence of carburizing time and carbon potential on D-coefficient value in Eq 10 (Ref 5)

applies to variant 1 and 8 of heat treatment and is compared to noncarburized bearing steel. Hardness measured with Rockwell and with Vickers methods shows a rapid increase for C content of 1.6%. Over this content, the increase is slight, and for some heat treatment variants, it is stabilized at a constant level (Fig. 11). Variant 2 at the surface C content 1.8 to 2.0% is the best method of heat treatment for samples 6 to 12 mm thick. Moreover, in the range of hardening temperatures from 1073 to 1123 K (800 to 850 °C), the hardness was invariable and independent of foundation material thickness. The growth of the foundation material thickness causes only insignificant decrease of hardness. From the viewpoint of used cooling medium, the oil at 393 K (120 °C) appears the best and is convenient to the traditional method of cooling bearing steel.

From these results, the carburizing process considerably improves volumetric fatigue strength and hardness in comparison with noncarburized bearing steel after traditional treatment. The best effects were given after carburizing at a surface content of 1.8 to 2.0 % C. In these conditions, the smallest contact fatigue (Fig. 12) and the lowest abrasive wear (Fig. 13) were obtained. It is related to the most beneficial compressive stresses (Fig. 14) and to the smallest value of Young's modulus (Fig. 15). The influence of C content on bending strength, tensile strength, and impact strength is presented in Fig. 16 to 18. An increase of more than 1% C (in all cross sections) is accompanied by a decrease in tensile, bending, and impact strength.

3.3 *Conclusions*

The carburized layer formed on elements made of LH15 steel increases considerably their functional properties. Results indicate that the highest utilizable properties (limited volumetric fatigue strength, hardness, contact fatigue life, abrasive wear intensity) of carburized low-chromium hypereutectoid LH15 (52100) steel can be obtained for 1.8 to 2.0% of the C content in the upper zone of the layer. It is related to the most beneficial compressive stresses, to the highest retained austenite participation (Ref 3), and to the lowest critical cooling rate (Ref 18). For higher contents of C, utilizable properties of the diffusion layers on LH15 steel are decreased. An increase of more than 1% C (in all cross sections) is accompanied by a decrease in tensile, bending, and impact strength.

The knowledge of the thermodynamic and kinetic analysis of the carburizing process in the two-phase fields (austenite-cementite) at 1173 K makes possible controlled carburizing of LH15 grade bearing steel. The C concentration at the surface obtained by a C potential of 1.2% C corresponds with the best functional properties of carburized LH15 (52100) steel. In section 4, the model of chemical and phase composition calculations for carburized layers formed on LH15 (52100) steel is presented.

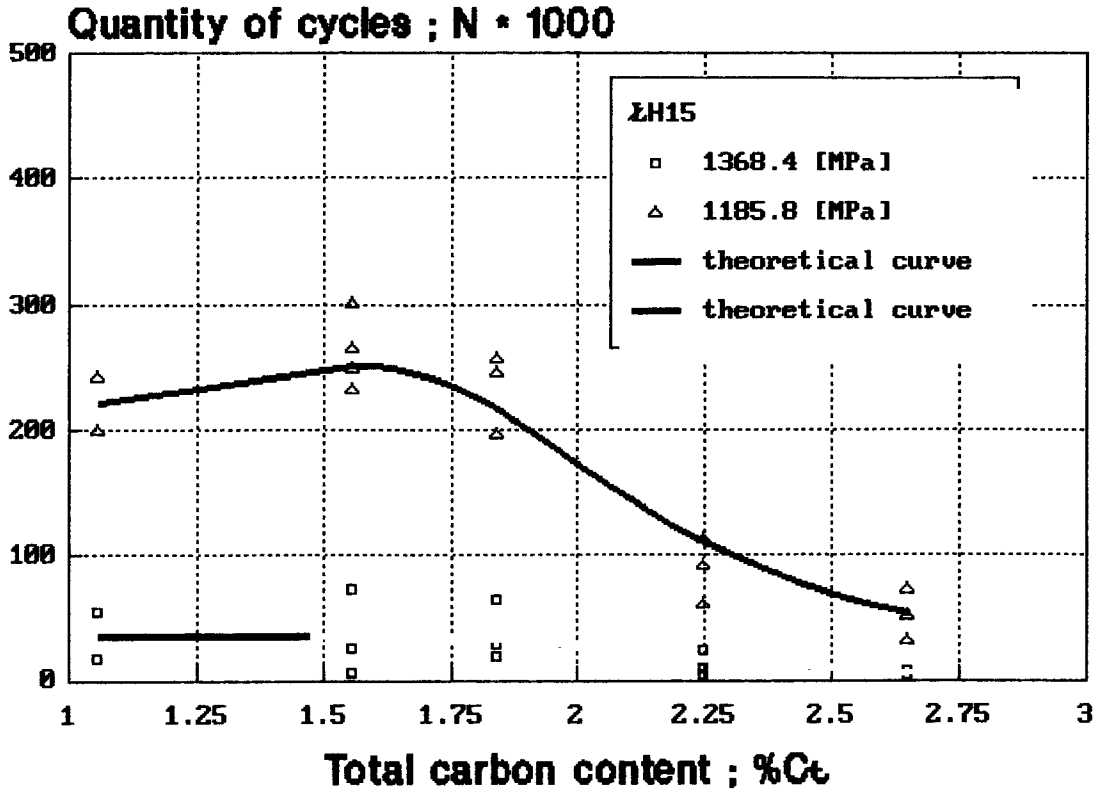

Fig. 10 Fatigue life versus carbon concentration at different stress levels of LH15 steel (Ref 16, 17)

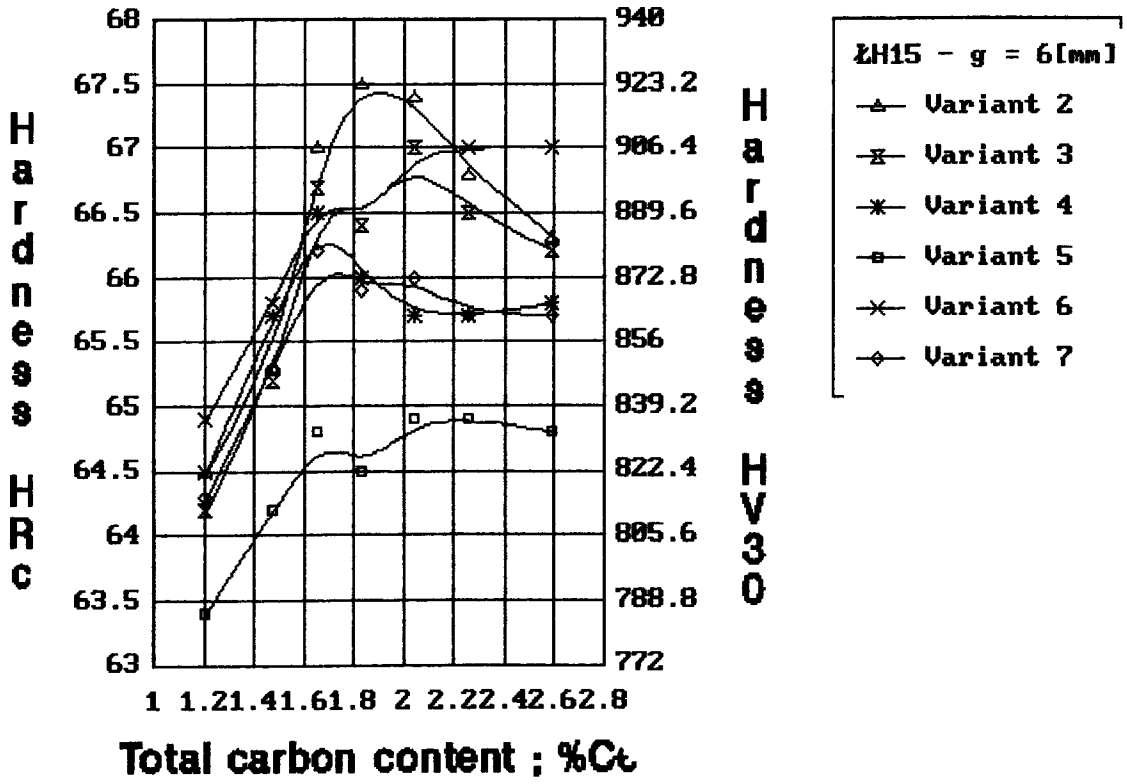

Fig. 11 Changes of hardness HRC and HV30 compared to total carbon content for carburized LH15 steel samples of 6 mm thickness after different heat treatments (according to Table 3) (Ref 16, 17)

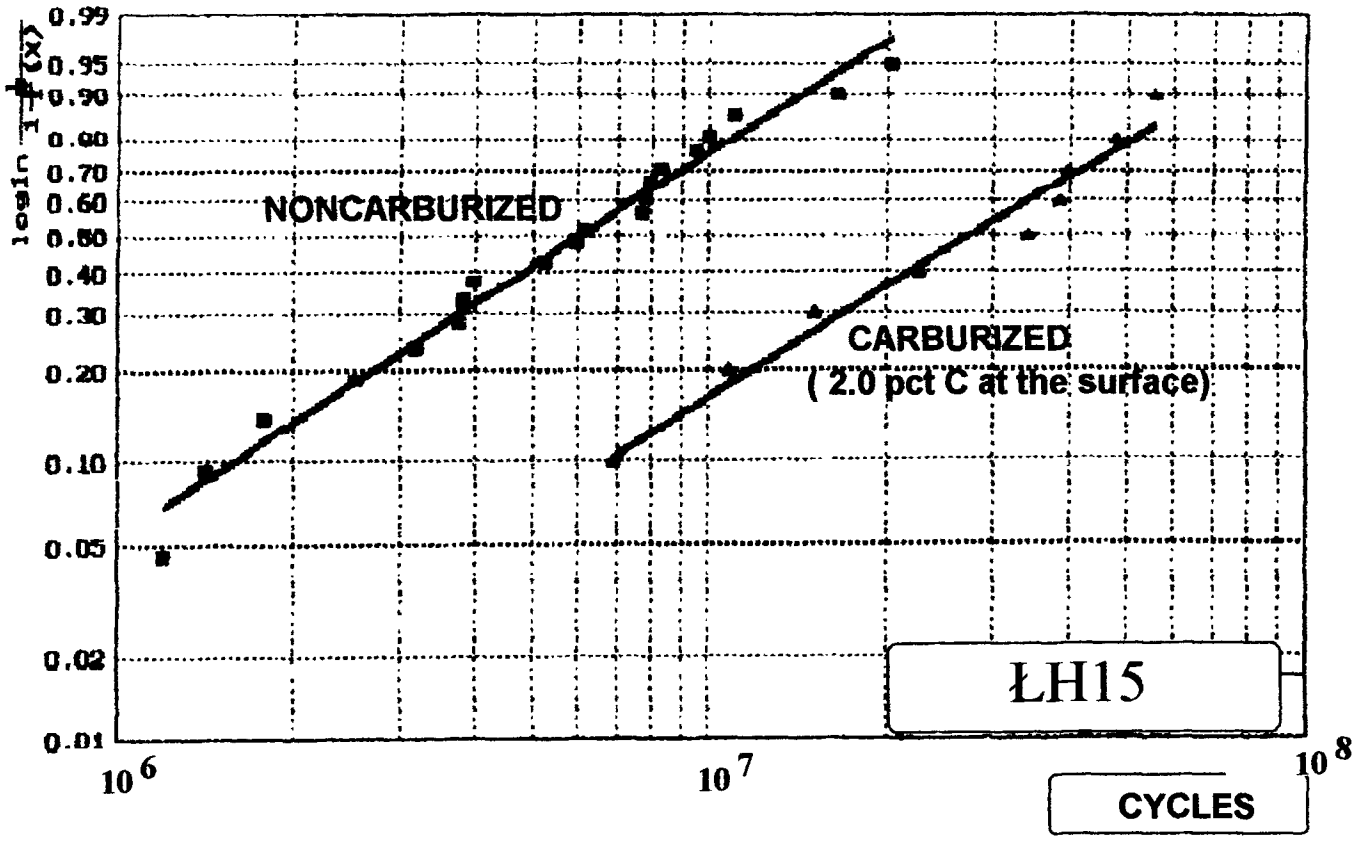

Fig. 12 Results of contact fatigue life investigations for LH15 bearing steel (Ref 1, 16). Variant 2 of heat treatment

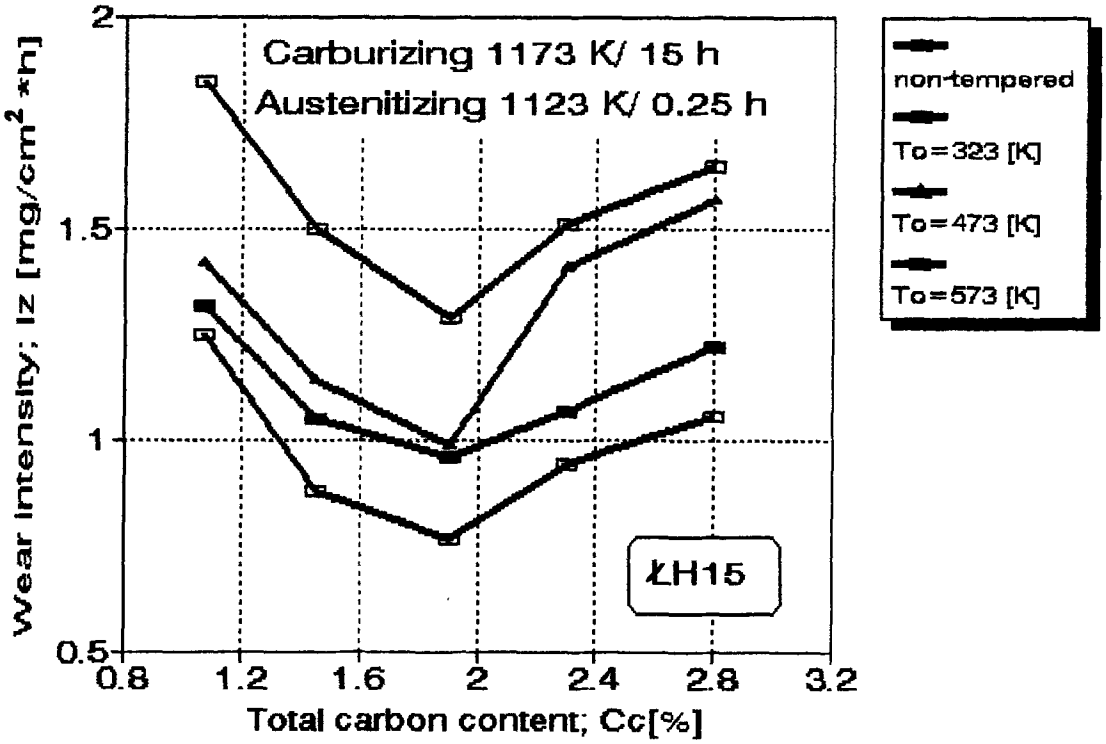

Fig. 13 Abrasive wear intensity versus surface carbon content of carburized LH15 steel (Ref 1, 16)

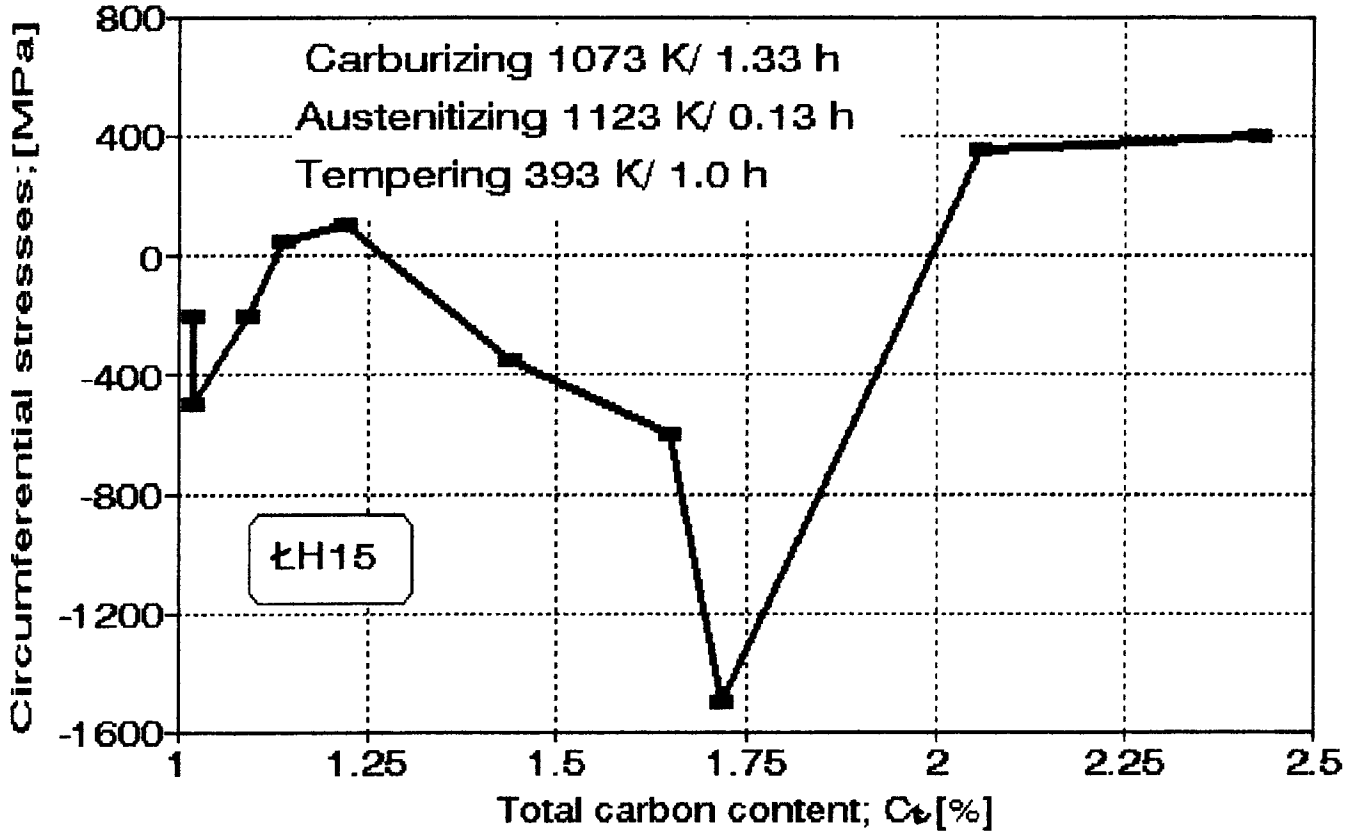

Fig. 14 Variation of circumferential stresses with subsurface layer carbon content for carburized LH15 steel (Ref 20)

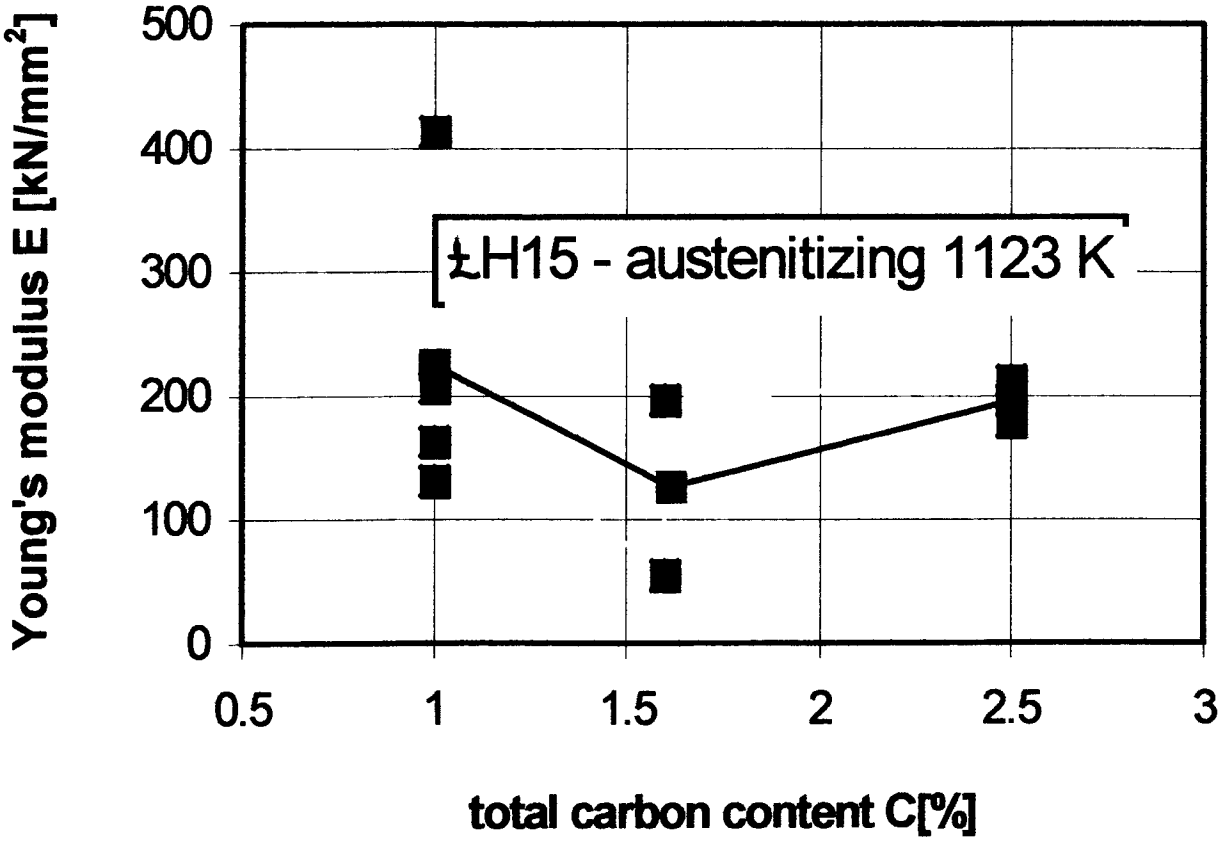

Fig. 15 Influence of carbon content on Young's modulus for LH15 steel

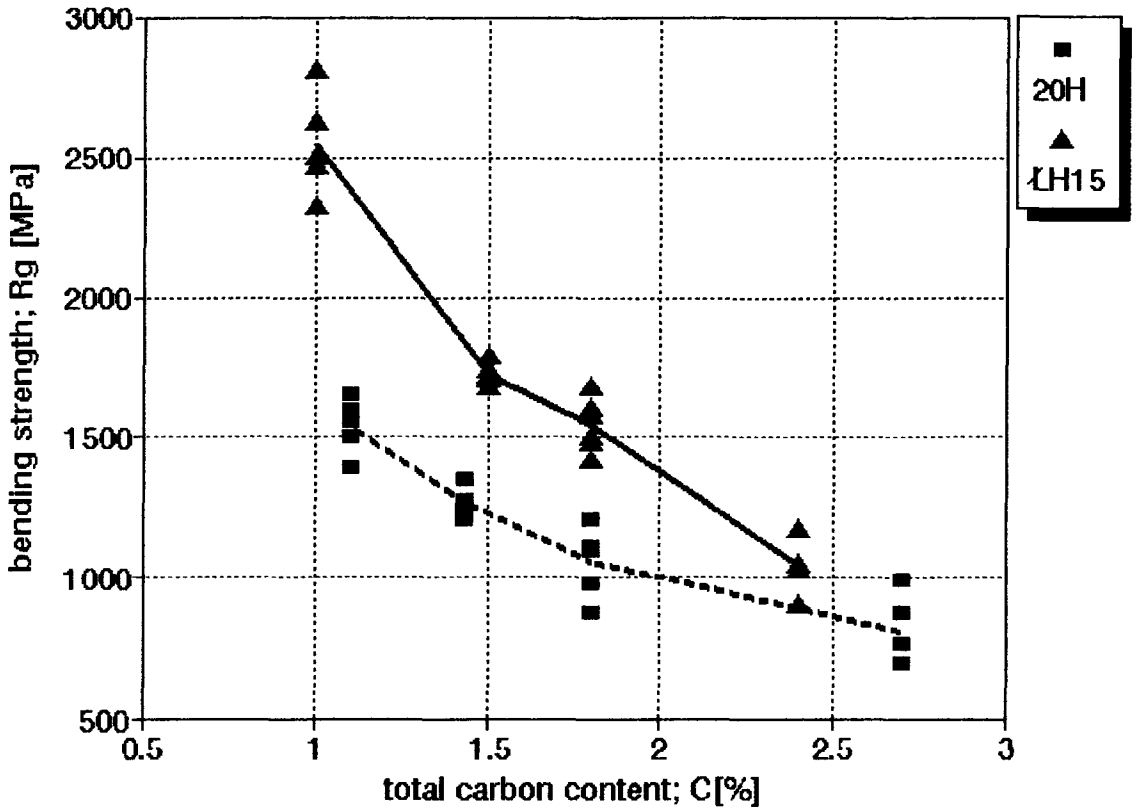

Fig. 16 Influence of carbon content on the bending strength of 20H and LH15 steels (Ref 19)

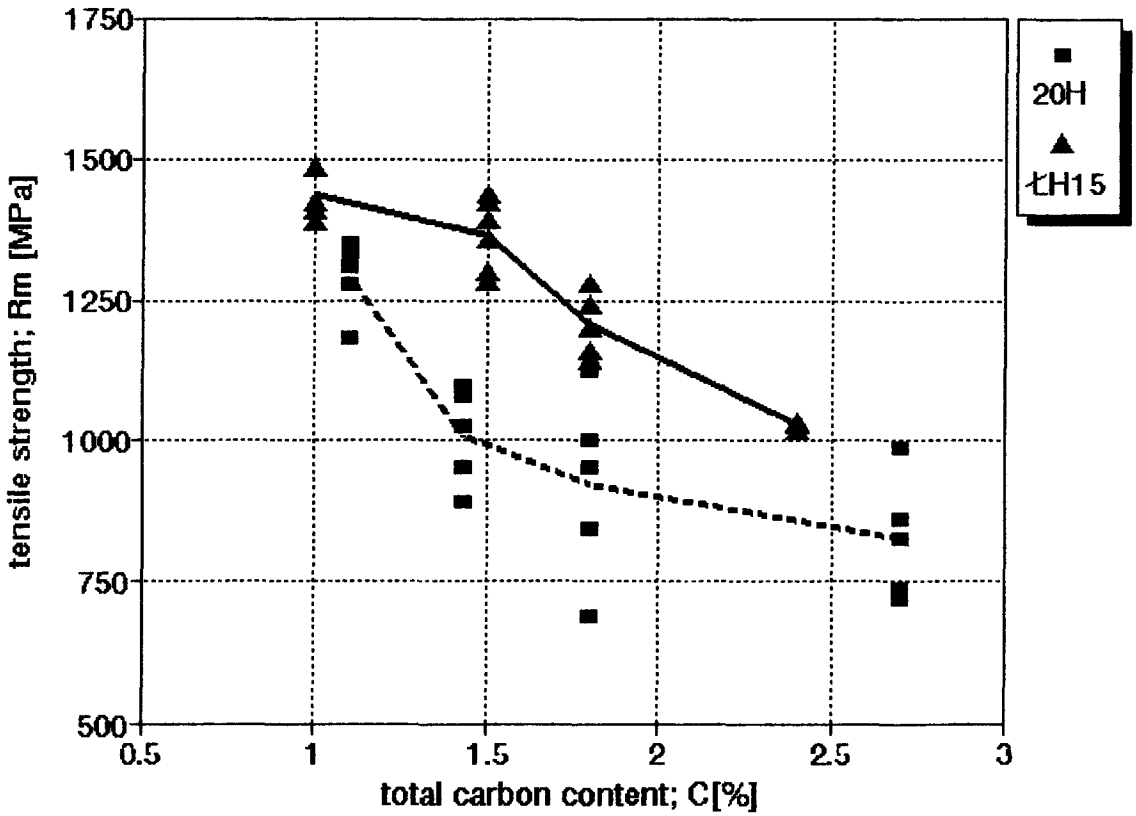

Fig. 17 Influence of carbon content on the tensile strength of 20H and LH15 steels (Ref 19)

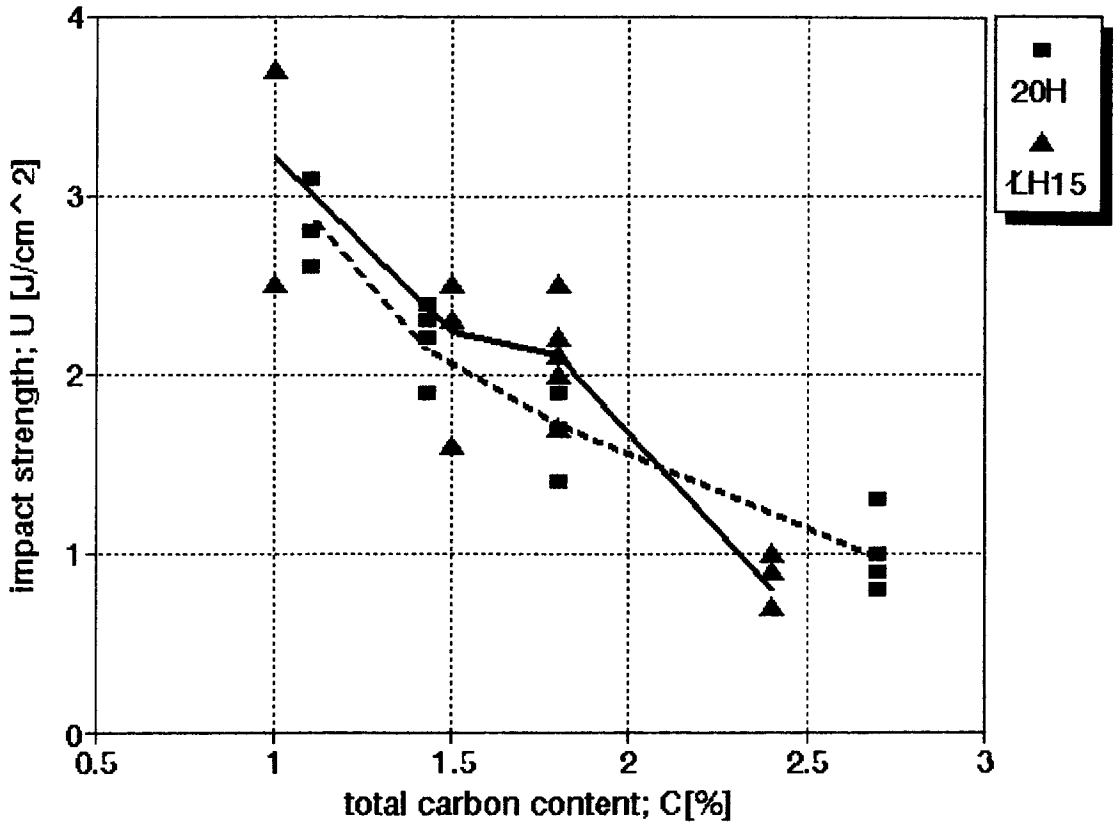

Fig. 18 Influence of carbon content on the impact strength of 20H and LH15 steels (Ref 19)

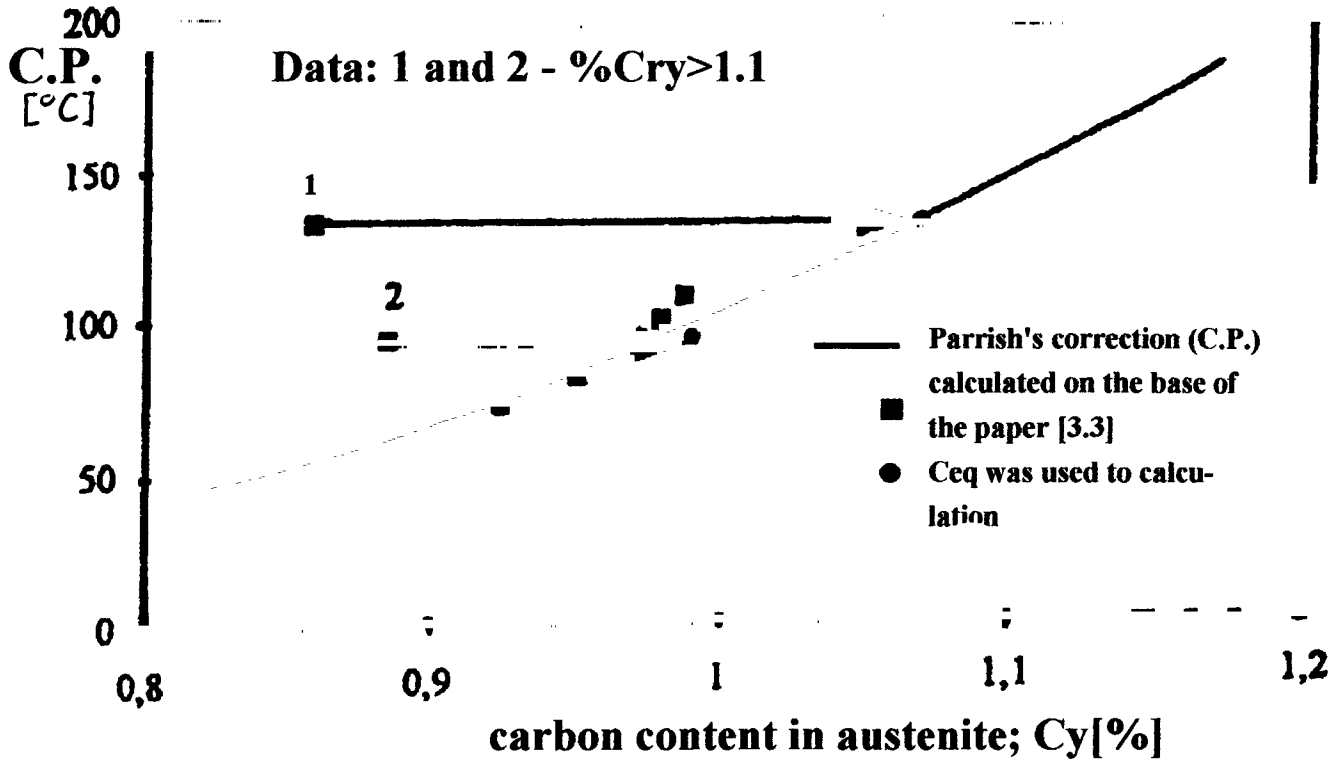

Fig. 19 Influence of carbon content in austenite on the Parrish correction (CP) and calculated results for LH15 (52100) steel based on retained austenite participation (Ref 7)

4. Calculation Model and Investigation Results of Chemical and Phase Composition of Carburized Low-Chromium Hypereutectoid Steels

The knowledge of thermodynamic and kinetic analysis of the carburizing process in the two-phase fields (austenite-cementite) at 1173 K enables controlled carburizing of LH15 (52100) bearing steel. The influence of the carburizing process on the functional properties of this material is described in section 3.

Many investigators were concerned with the influence of C content on chemical and phase composition of carburized layers formed on low-chromium hypereutectoid steels. The results of most investigators agree with the calculation model described in Ref 7. This model was used to determine chemical and phase composition for carburized layers formed on LH15 (52100) steel. The model for fixed carburizing and austenitizing parameters together with existing experimental data is presented here.

4.1 *Experimental Procedure and Calculation Model*

According to PN-74/H-84041 (Table 2), investigation results are related to chemical composition of used LH15 (52100) bearing steel. The carburized layers in this steel were formed by controlled carburizing atmospheres at 1173 K according to the experimental procedure presented in section 2. Figures 5 to 7 present the dependence of the total C content variations versus the distance from the surface of carburized bearing steel. Samples with different total surface C contents for investigations were prepared based on Fig. 5 to 7. The samples were heat treated (hardened and tempered). The austenitizing temperature 1123 K (850 °C) and tempering temperature 423 K (150 °C) were used. The Cr concentration in martensitic matrix and in cementite was examined with the aid of the x-ray microanalyzer (Ref 1). Participations of retained austenite and cementite in carburized layer were determined using the Mössbauer method and x-ray diffraction methods (Ref 3). The influence of the total C content on the martensitic transformation start temperature was determined by dilatometric analysis (Ref 18). Dilatometric samples were carburized and annealed in vacuum to obtain homogeneous C content in all cross sections. These samples with different C content were quenched from 1113 K (840 °C). The position of transformation curves of martensite and bainite was established.

In Ref 7, the calculation model of chemical and phase composition of carburized layers formed on low-chromium hypereutectoid steels was presented. The influence of the total C content in carburized layer on LH15 (52100) steel on Cr and C contents in austenite was described (Ref 3). The solubility of carbides for Fe-C alloys is approximately expressed as:

$$Acm_o = -0.74 + 2.05\ 10^{-3}\ T \qquad \text{(Eq 13)}$$

where T is temperature in °C.

For Fe-Cr-C alloys, the solubility of carbides was calculated using Eq 14 (Ref 7):

$$Acm_{Cro} = Acm_o - \frac{Cr_t}{10} \qquad \text{(Eq 14)}$$

where Cr_t is total chromium content in wt%.

In described carburized layers formed on hypereutectoid steels, the Cr content in austenite (in martensite after hardening) falls together with increasing of the total C content due to the partial solubility of Cr in cementite. Consequently, the C content in austenite (corresponding to solubility of carbides) increases and is given by Eq 15 (Ref 7):

$$Acm = Acm_o - \frac{Cr_t}{10} \exp\left[-(C_t - Acm_{Cro})\right] \qquad \text{(Eq 15)}$$

where C_t is total carbon content in wt%.

Participation of cementite is expressed as (Ref 7):

$$F_{cm} = \frac{C_t - Acm}{6.72 - Acm} \qquad \text{(Eq 16)}$$

where 6.72 is the mean value of C content in cementite (wt%) by total carbon content C_t from 1.1 to 2.7 (wt%).

The start temperature of martensitic transformation is calculated based on the Steven-Hayes equation (Ref 21) modified by Parrish (Ref 22):

$$M_s = 561 - 474\ C - 33\ Mn - 17\ Cr - 17\ Ni - 21\ Mo + CP \qquad \text{(Eq 17)}$$

M_s is martensitic transformation start temperature (°C); C is carbon content in austenite (wt%); Mn is manganese content in austenite (wt%); Cr is chromium content in in austenite (wt%); Ni is nickel content in austenite (wt%); Mo is molybdenum content in austenite (wt%); and CP is the Parrish correction (°C).

For Fe-Cr-C alloys, the influence of C and Cr content in austenite on M_s temperature is consequently given by:

$$M_s = 552 - 474\ C_{\gamma Cr} - 17\ Cr_\gamma + CP \qquad \text{(Eq 18)}$$

where $C_{\gamma Cr}$ is carbon content in austenite of Fe-Cr-C alloy (wt%), and Cr_γ is chromium content in austenite of Fe-Cr-C alloy (wt%).

Participation of retained austenite is expressed by the Koistinen-Marburger relation (Ref 23):

$$Fe_\gamma = (1 - F_{cm}) \exp\left(-1.1 \times 10^{-2}\left[M_s - T_Q\right]\right) \qquad \text{(Eq 19)}$$

where Fe_γ is participation of retained austenite; M_s is martensitic transformation start temperature (°C); Fe_{cm} is participation of cementite; and T_Q is cooling liquid temperature (°C).

According to expectation, after hardening of the carburized layer on low-chromium hypereutectoid steel the following phases exist: martensite, cementite, and retained austenite. For the C content, higher than 0.5 wt% Parrish's correction (CP) was used to determine the M_s temperature. In Ref 7, this correc-

tion was presented on the basis of existing investigations (Ref 1, 3). Using Eq 19 to determine M_s temperature, it is possible to calculate CP on the basis of Eq 18. Experimental data of retained austenite participation were used to calculate the Parrish correction. The results obtained are presented in Fig. 19. For Cr content in austenite (in martensite after hardening) higher than 1.1 wt%, equivalent C content C_{eq} (wt%) was used to calculate:

$$C_{eq} = C_{\gamma Cr} + 0.7\,(Cr_\gamma - 1.1) \qquad \text{(Eq 20)}$$

Chromium content in austenite is calculated using Eq 21 and 22:

$$Cr_\gamma = \frac{Cr_t}{1 - F_{cm}(1 - \tau)} \qquad \text{(Eq 21)}$$

$$\tau = \frac{Cr_{cm}}{Cr_\gamma} \qquad \text{(Eq 22)}$$

where τ is partition coefficient of Cr between austenite and cementite determined in Ref 24, and Cr_{cm} is Cr content in cementite (wt%).

Figure 20 presents the influence of austenitizing temperature on partition coefficient of Cr between austenite and cementite. In thermodynamic equilibrium conditions, this value depends on temperature. It was assumed that, for carburized layer formed on LH15 (52100) steel, the equilibrium between austenite and cementite was approximately reached.

4.2 *Investigation and Calculation Results*

Table 4 presents calculation results of chemical and phase composition of the carburized layer formed on low-chromium hypereutectoid LH15 (52100) steel for austenitizing temperature 1123 K (850 °C). Results show that the best effects were obtained after carburizing at the surface C content ranging from 1.8 to 2.0%. Phase analysis shows that at these C contents, about 20% of retained austenite (Fig. 21) and 17% of cementite (Fig. 22) exists in carburizing bearing steels. It is related to the

Table 4 Chemical and phase composition of carburized layer of LH15 steel hardened from 1123 K (850 °C)

C_t, %	Acm, %	F_{cm}, %	Cr_γ, %	CP, °C	M_s, °C	Fe_γ, %
1	0.878	2.08	1.237	120	235	9.2
1.2	0.901	5.14	1.032	96	204	12.5
1.6	0.934	11.51	0.767	80	177	15.7
2	0.957	18.10	0.607	87	175	14.9
2.4	0.972	24.85	0.499	92	175	13.7
2.8	0.982	31.68	0.424	98	178	12.0
3.2	0.989	38.58	0.367	100	177	10.0

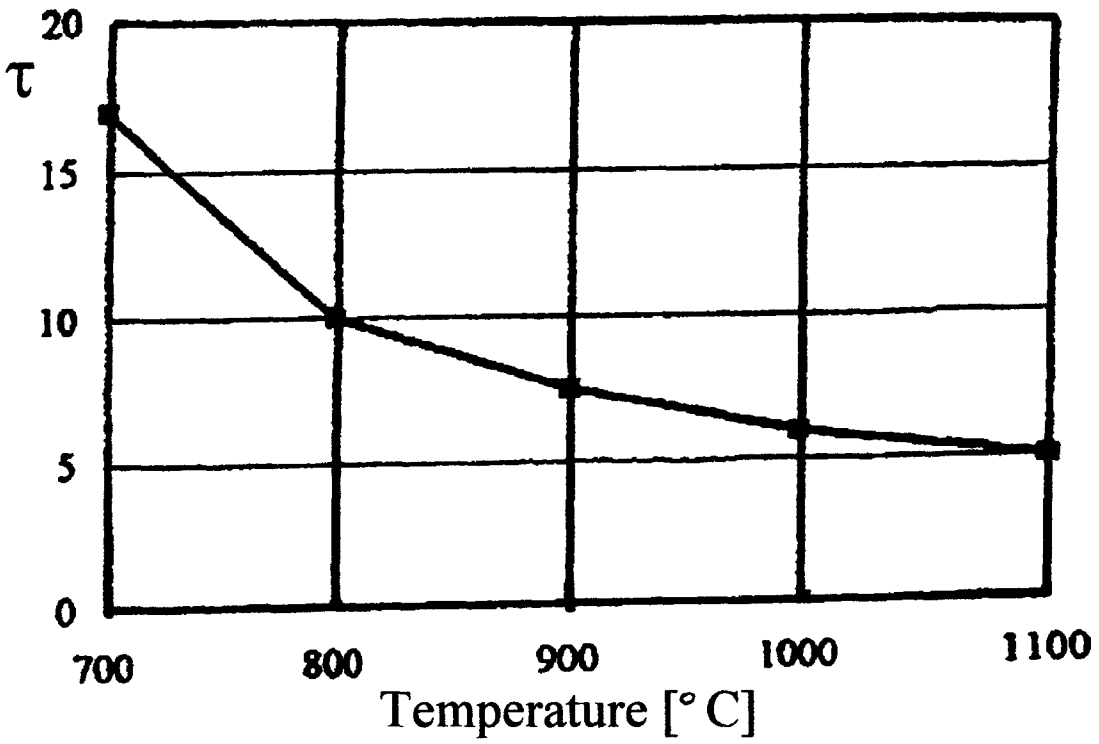

Fig. 20 Partition coefficient of chromium between austenite and cementite as a function of temperature (Ref 24)

lowest martensitic transformation beginning temperature (M_s) and to the lowest critical cooling rate (Fig. 23). Figure 21 presents the changes of retained austenite in carburized layer on LH15 steel. Research shows that the highest participation of retained austenite is accompanied by 1.8% C content. The experimental data agree with the calculation curve.

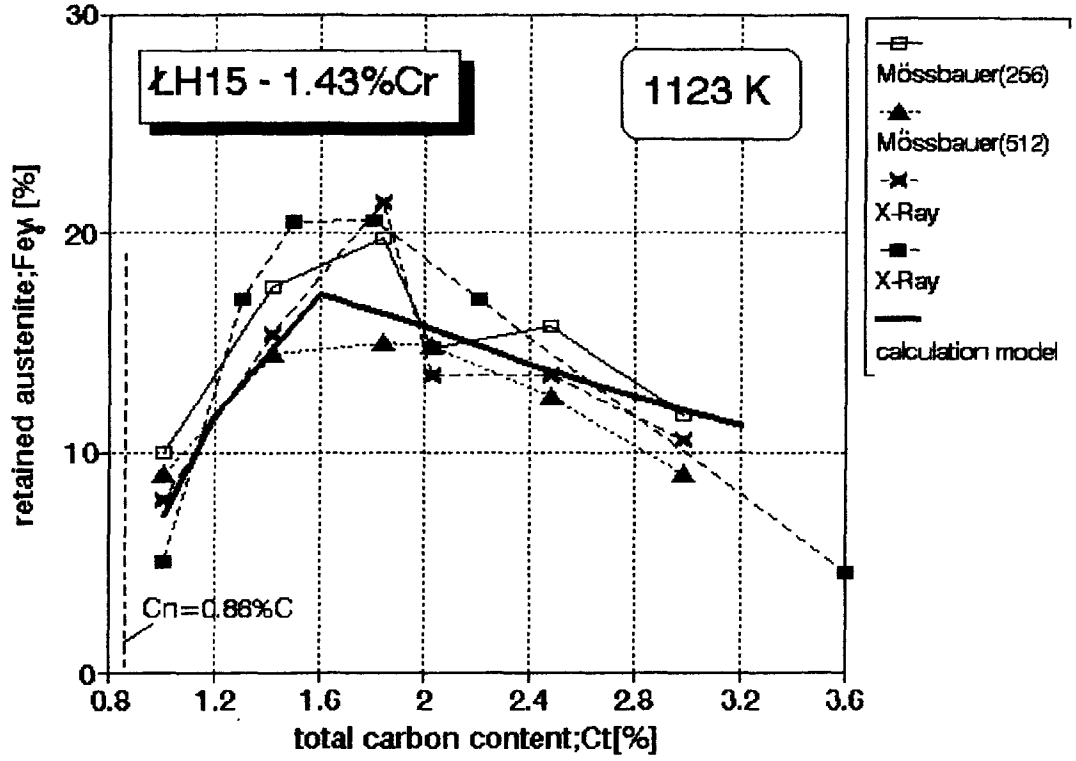

Fig. 21 Influence of carbon content on the participation of retained austenite in carburized, hardened, and tempered bearing LH15 (52100) steel. Austenitizing temperature: 1123 K (850 °C)

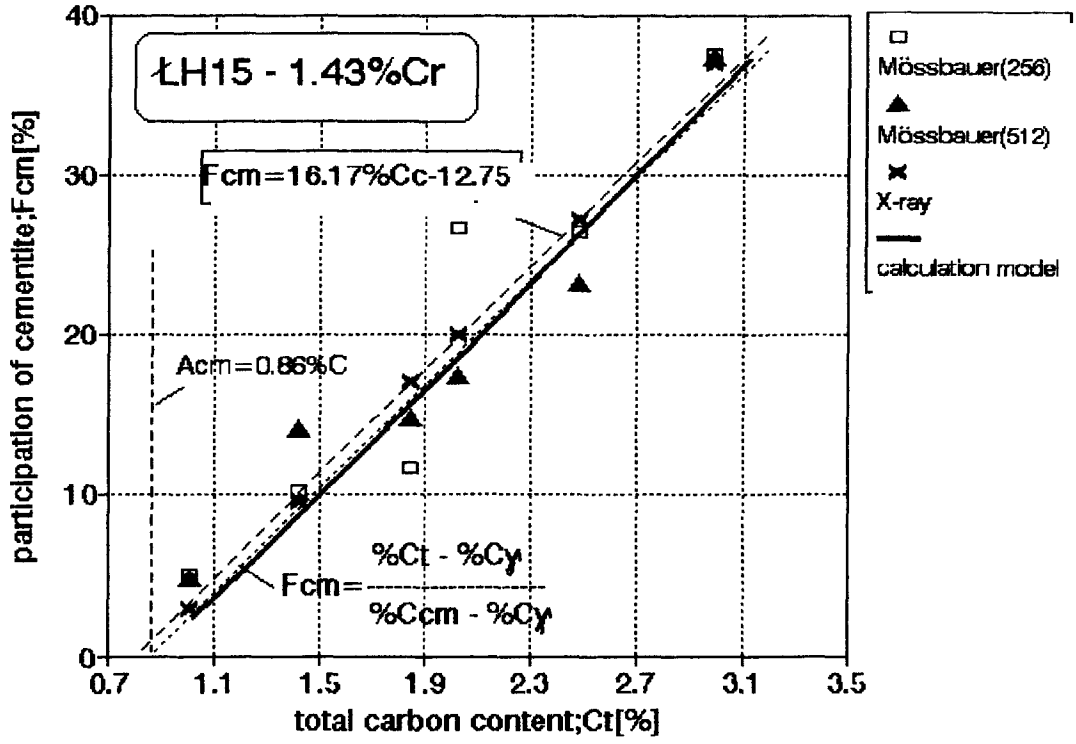

Fig. 22 Influence of carbon content on the participation of cementite in carburized and heat treated LH15 (52100) steel (variant 2 in Table 3)

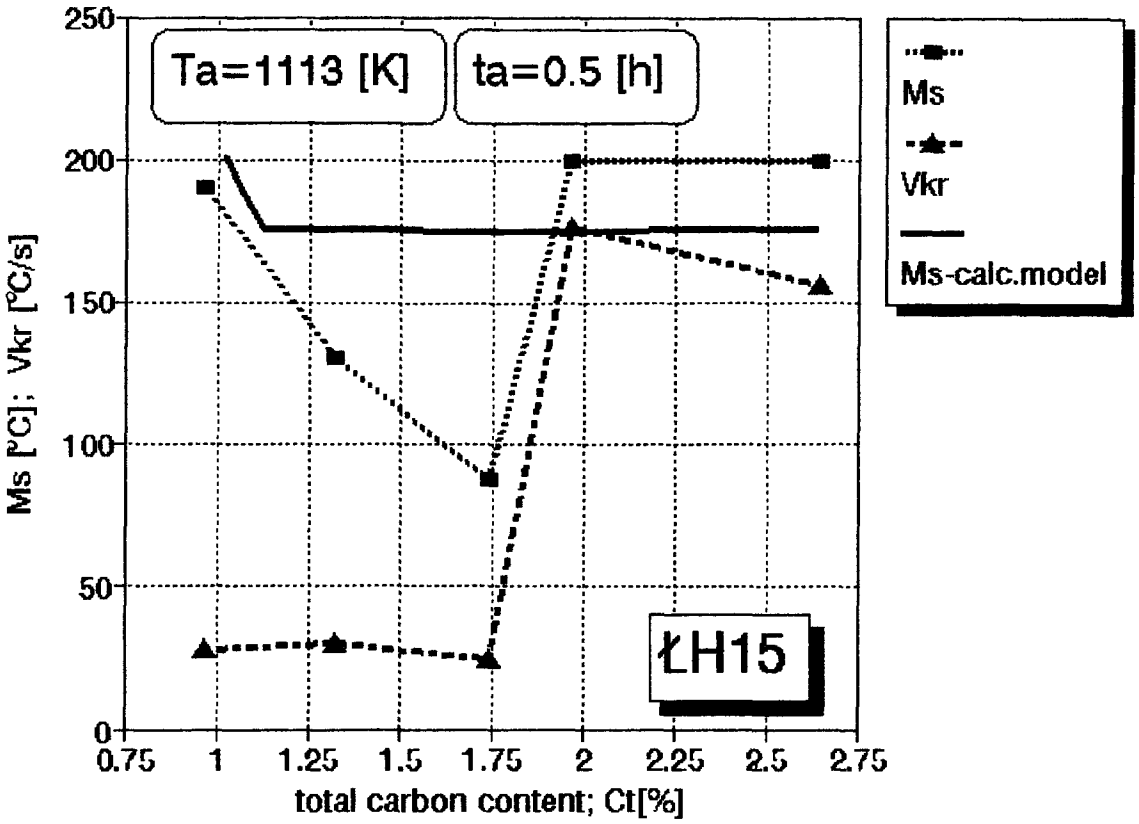

Fig. 23 Martensitic transformation start temperature (M_S) and critical cooling rate (Vkr) versus carbon content for carburized LH15 steel (Ref 18)

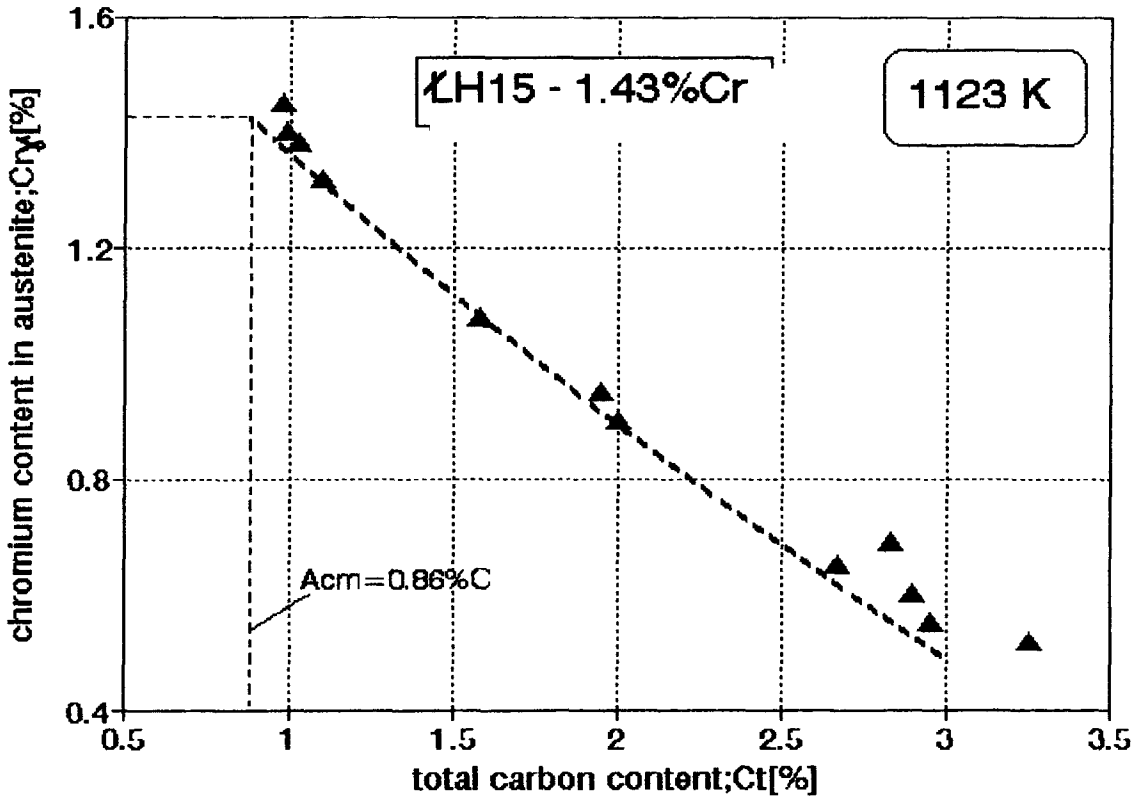

Fig. 24 Influence of carbon content on chromium content in austenite (in martensitic matrix) in carburized and heat treated LH15 (52100) steel (variant 2 in Table 3)

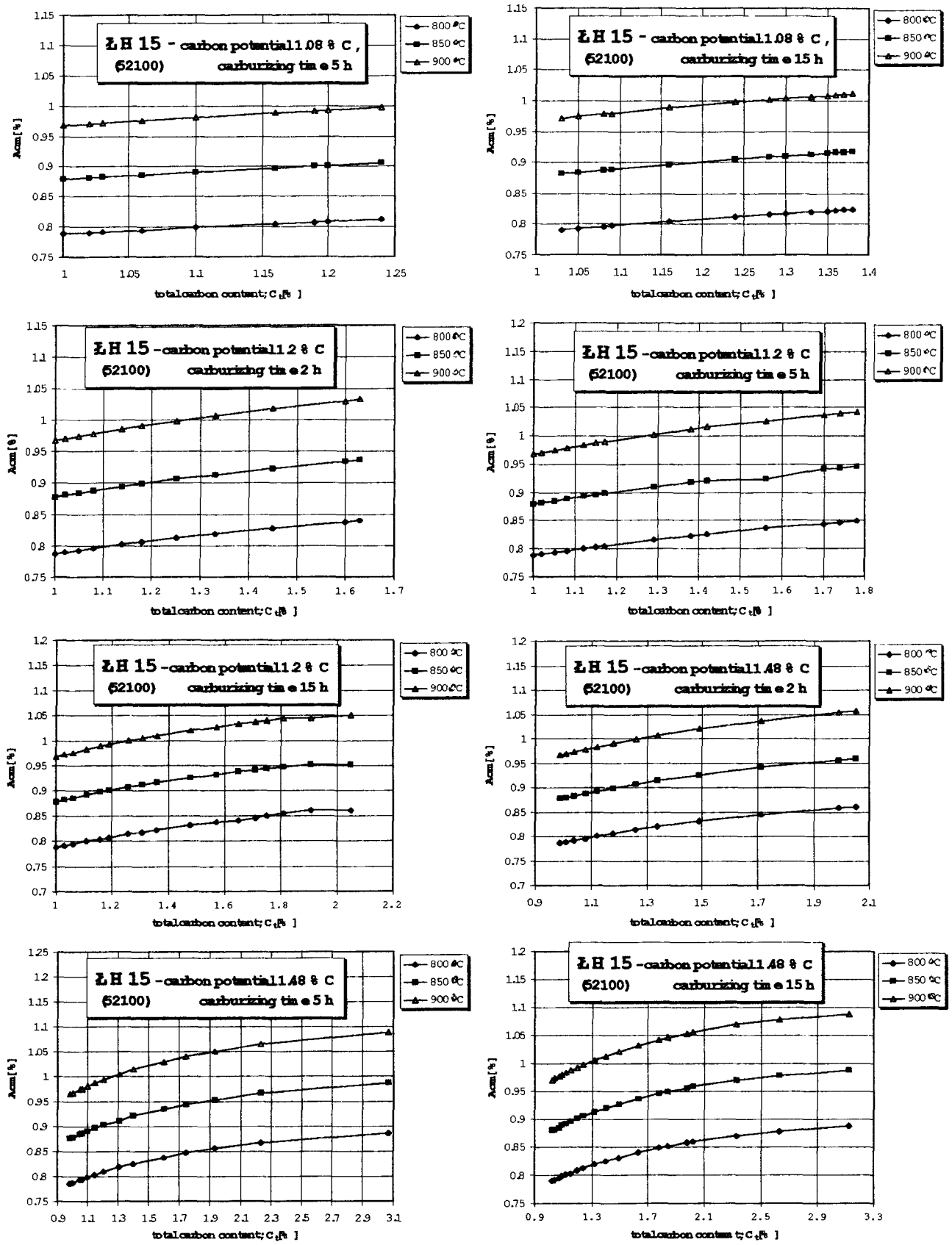

Fig. 25 Influence of total carbon content C_t and austenitizing temperature (800, 850, 900 °C) on carbon content in austenite (in martensitic matrix after hardening) Acm in carburized layer formed on LH15 (52100) steel by fixed carburizing parameters (carburizing temperature, 900 °C)

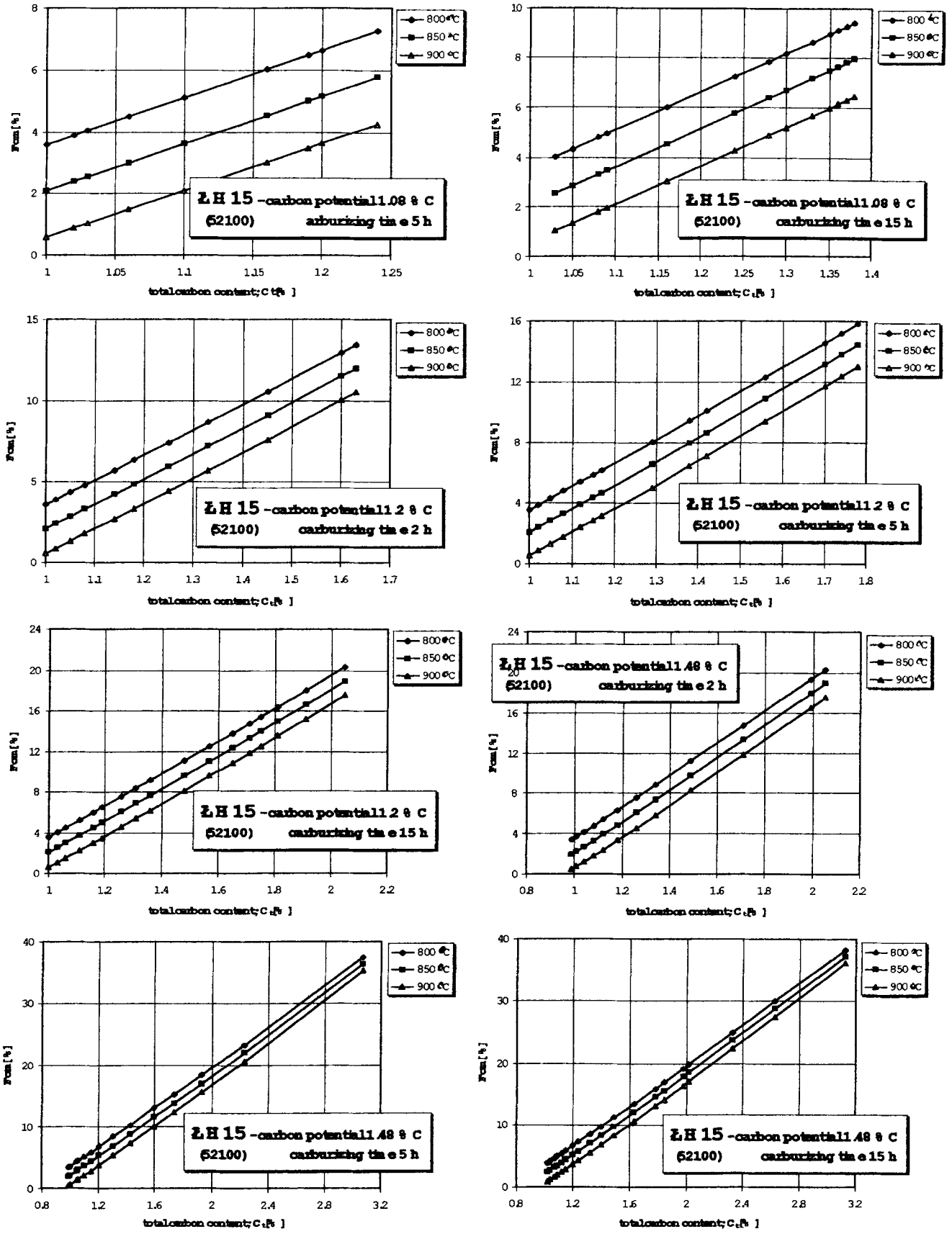

Fig. 26 Influence of total carbon content C_t and austenitizing temperature (800, 850, 900 °C) on cementite participation F_{cm} in carburized layer formed on LH15 (52100) steel by fixed carburizing parameters (carburizing temperature, 900 °C)

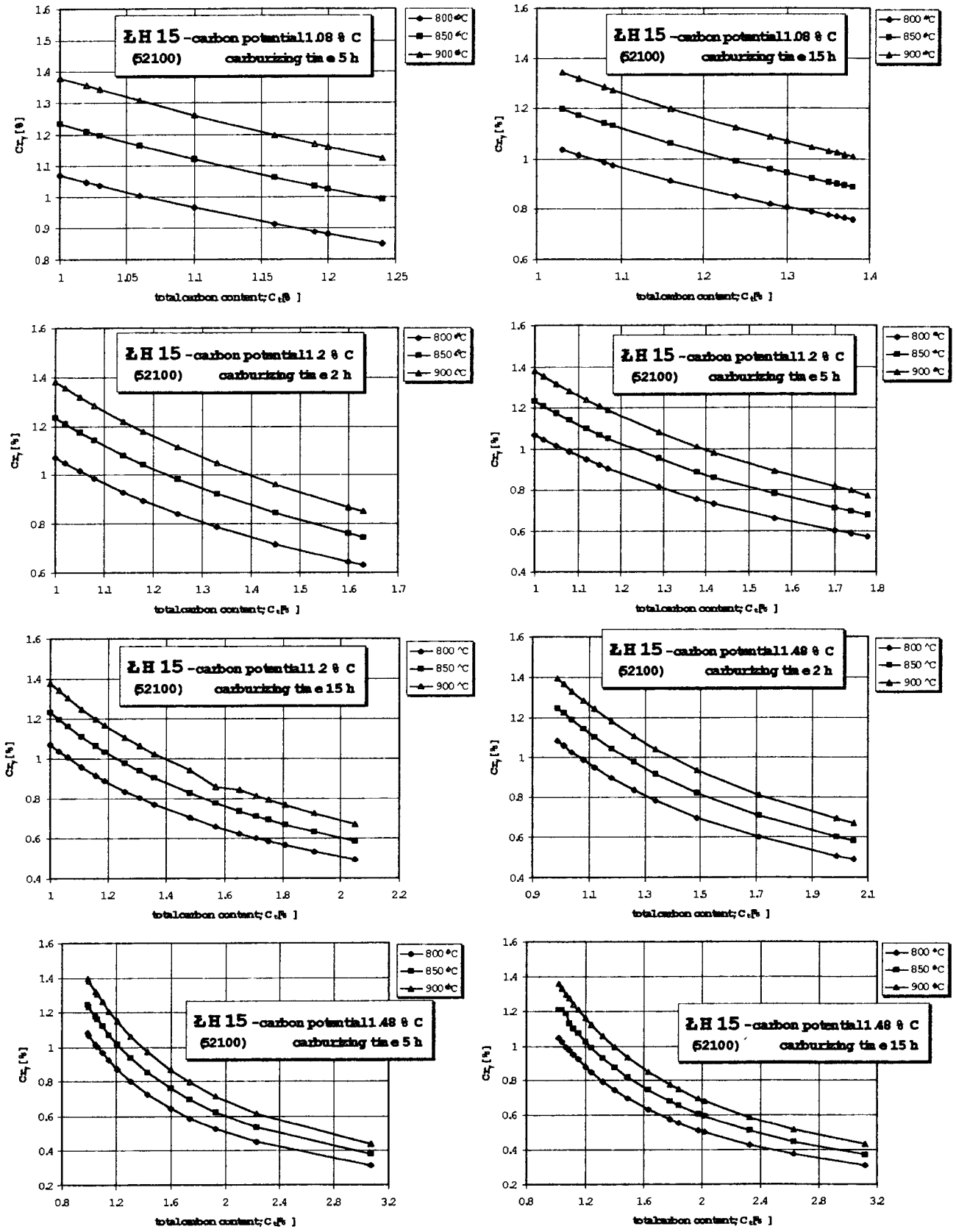

Fig. 27 Influence of total carbon content C_t and austenitizing temperature (800, 850, 900 °C) on chromium content in austenite (in martensitic matrix after hardening) Cr_γ in carburized layer formed on LH15 (52100) steel by fixed carburizing parameters (carburizing temperature, 900 °C)

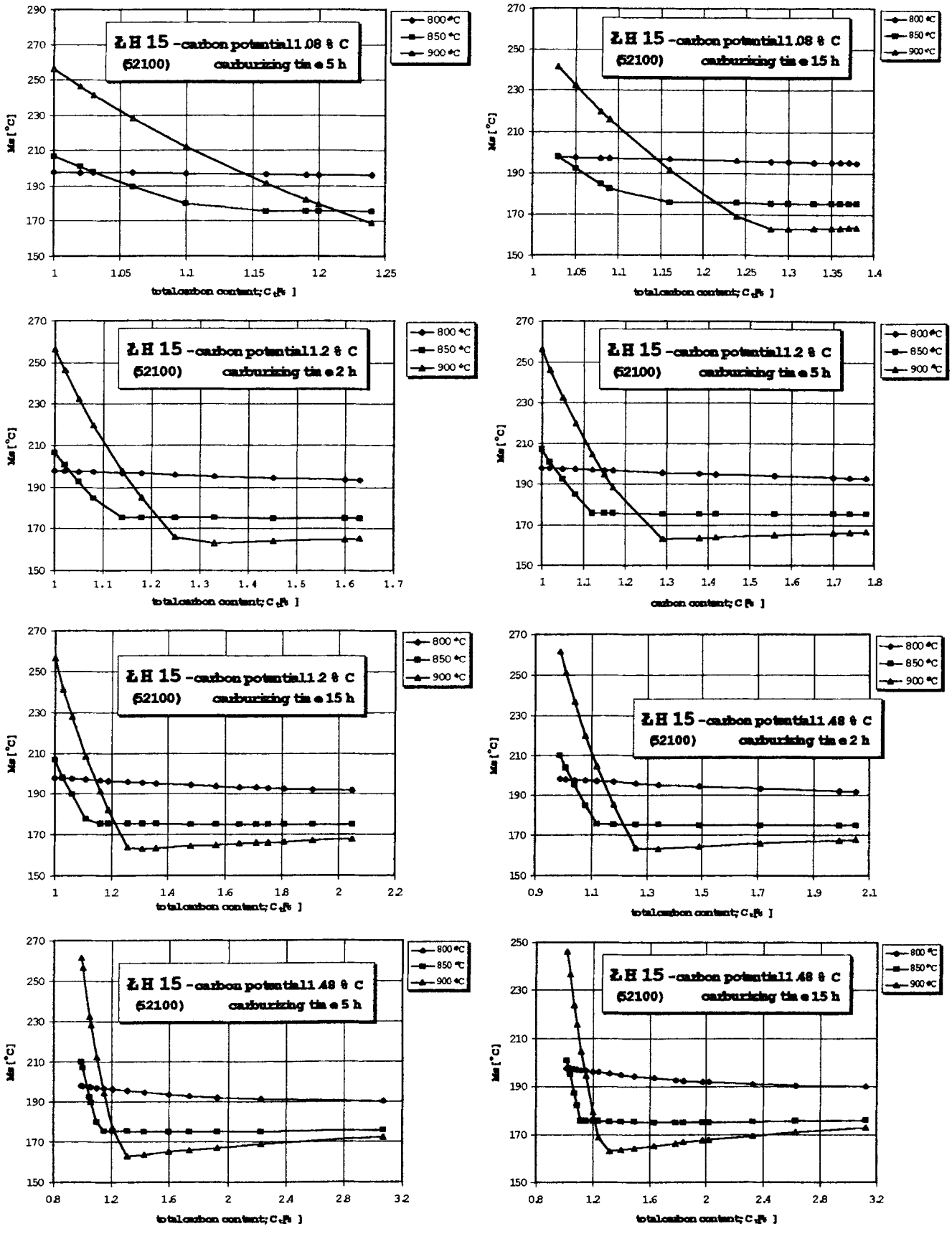

Fig. 28 Influence of total carbon content C_t and austenitizing temperature (800, 850, 900 °C) on martensite transformation start temperature, M_S, in carburized layer formed on LH15 (52100) steel by fixed carburizing parameters (carburizing temperature, 900 °C)

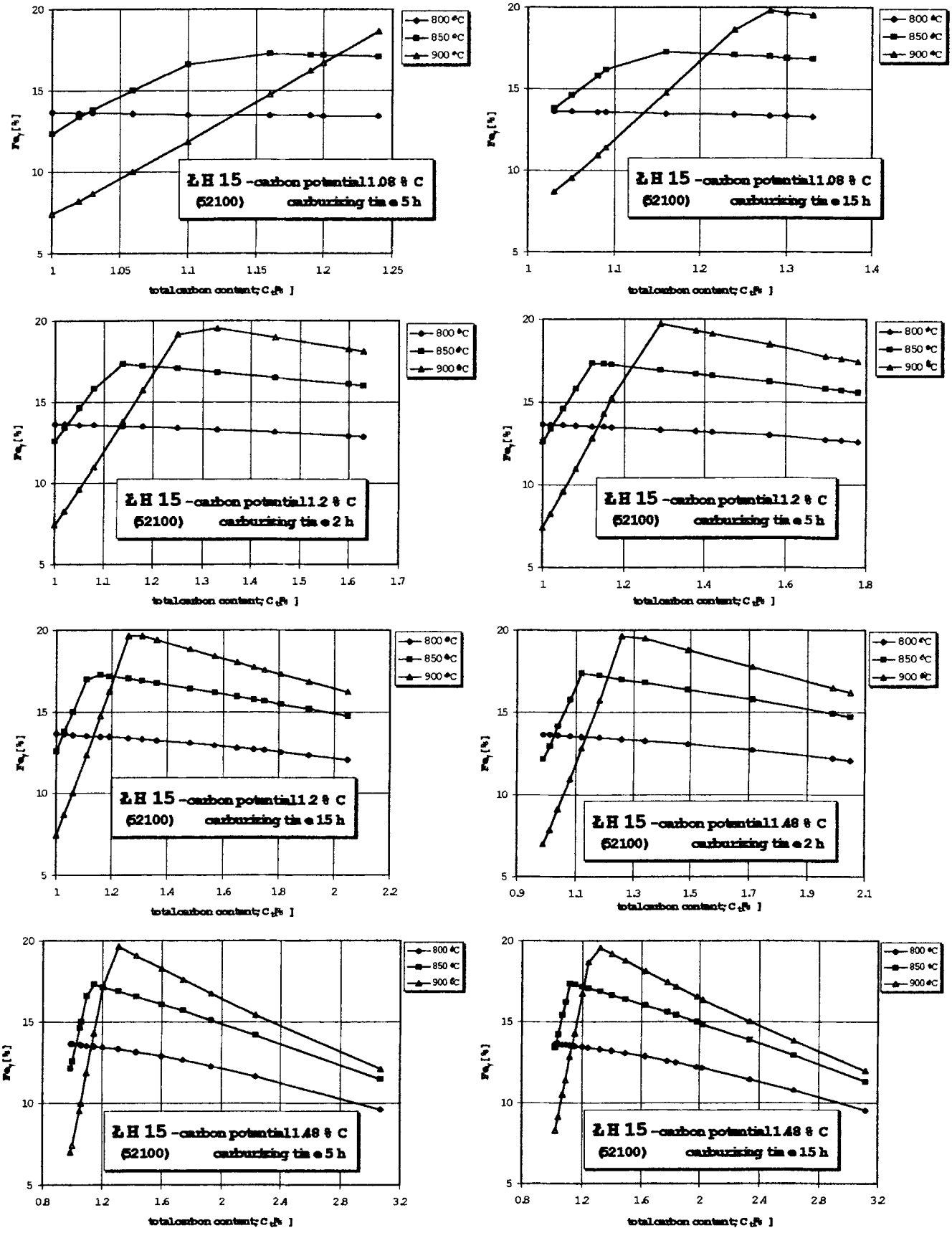

Fig. 29 Influence of total carbon content C_t and austenitizing temperature (800, 850, 900 °C) on retained austenite participation Fe_γ in carburized layer formed on LH15 (52100) steel by fixed carburizing parameters (carburizing temperature, 900 °C)

Figure 22 presents the influence of the total C content on the cementite participation. Increasing of total C content is accompanied by increasing of cementite participation. The experimental data obtained by the Mössbauer method and XRD were analyzed by the following calculation procedures: linear regression and the knowledge of the chemical composition of austenite and cementite (wt% C). Results are represented by straight lines and agree with those obtained by the presented model (solid line in Fig. 22).

Changes of martensitic transformation start temperature, M_s, and critical cooling rate, Vkr, as a function of the total C content are presented in Fig. 23. Experimental and calculation data show that the lowest M_s temperature and critical cooling rate were obtained at 1.8% C in carburized layer.

Increasing of total C content is accompanied by decreasing of Cr in austenite (in martensitic matrix after hardening). Figure 24 shows experimental data (Ref 1). Figure 24 shows that at 1.8% C in martensitic matrix, there exists about 0.95% Cr.

Other figures show the calculated results of chemical and phase composition according to the model under consideration. Three various austenitizing temperature and the following calculation procedure were used:

1. Calculation of C content in austenite, Acm (corresponding to solubility of carbides). Equations 19 to 21 were used.
2. Calculation of cementite participation, F_{cm}, according to Eq 16
3. Calculation of Cr content in austenite, according to Eq 21 and 22
4. Calculation of martensitic transformation start temperature, M_s, according to Eq 18
5. Calculation of retained austenite participation, Fe_γ, according to Eq 19

The carbon profiles of the layers on LH15 (52100) steel presented in Fig. 5 to 7 were used in calculations. The following carburizing parameters were applied: (a) temperature 1173 K (900 °C); (b) carbon potential 1.08% C and two carburizing times, 5 and 15 h; (c) carbon potential 1.2% C and three carburizing times, 2, 5, and 15 h; (d) carbon potential 1.48% C and three carburizing times, 2, 5, and 15 h.

Based on the elaborate methodology of calculations, the influence of the total C content in the carburized layer on the C content in austenite (in martensitic matrix after hardening) was determined. Results of the calculations for all C profiles obtained and for fixed austenitizing temperatures—1073 K (800 °C), 1123 K (850 °C), and 1173 K (900 °C)—are shown in Fig. 25. Figure 25 shows that increasing of total C content in carburized layer is accompanied by increasing of C concentration in austenite for all carburizing and austenitizing parameters. Higher values of C content in austenite were observed at higher austenitizing temperatures.

Results obtained from calculations of the changes of C concentration in austenite were utilized to determine the cementite participation in carburized layer. Participation of cementite, F_{cm}, in wt%, was calculated from Eq 16 and shown in Fig. 26. With increasing of the total C content and decreasing of the austenitizing temperature, cementite participation increases. The highest cementite participation at the surface of the carburized layer at high C potentials and long carburizing times was observed.

The influence of the total C content on Cr concentration in austenite (in martensitic matrix after hardening) is presented in Fig. 27. Increasing of the total C content and decreasing of the austenitizing temperature are accompanied by decreasing of the Cr content in austenite. It is related to partial solubility of Cr in cementite. The lowest values of the surface Cr content in austenite in carburized layer at high C potentials and long carburizing times were obtained due to the highest total C contents at the surface.

Figure 28 shows the calculated results of the martensitic transformation start temperature. The calculated data showed that the lowest M_s temperature was obtained by 1.8% of the total C in the carburized layer. With decreasing of the total C content, higher values of M_s temperature were observed. Starting from about 1.8% of total C content, a martensitic transformation start temperature in carburized layer increases. The bigger changes of M_s temperature as a function of the total C content at higher austenitizing temperatures were given.

Figure 29 shows the calculated results of the participation of retained austenite in relation to the total C concentration in carburized layer and austenitizing temperature. Data given show that retained austenite participation reaches its maximum values at the total C content amounting to about 1.1 to 1.8% C. The highest participation of retained austenite is accomplished by the lowest martensitic transformation start temperature, M_s. The maximum values of retained austenite participation at the surface of the carburized layer were obtained at the lowest C potentials and at higher austenitizing temperatures.

4.3 *Conclusions*

Participation of cementite and retained austenite in carburized layer on LH15 (52100) steel were defined using various methods of research and calculations. The relationship between the total C contents in the carburized layer and martensitic transformation start temperature and the C and Cr concentrations in austenite are also given. Examination results in section 3 show that the highest utilizable properties (limited volumetric fatigue strength, hardness, contact fatigue life, abrasive wear intensity) of LH15 (52100) steel can be obtained for 1.8 to 2.0% of C content in the upper zone of the layer. For higher contents, decreasing of utilizable properties in the diffusion layers on this steel is observed. For austenitizing temperature 1123 K (850 °C), the best functional properties of the layer are connected with the C and Cr concentrations in austenite at 0.93% C and 0.94% Cr and with the participation of cementite and of retained austenite of about 17% and 20%, respectively. It is related to the lowest martensitic transformation start temperature, M_s, to the lowest critical cooling rate, and to the most beneficial compressive stresses.

The thermodynamic and kinetic model of carburizing in two-phase fields presented in section 2 and the calculated model of chemical and phase composition can be used to model the structure and properties by controlled carburizing and heat treatment.

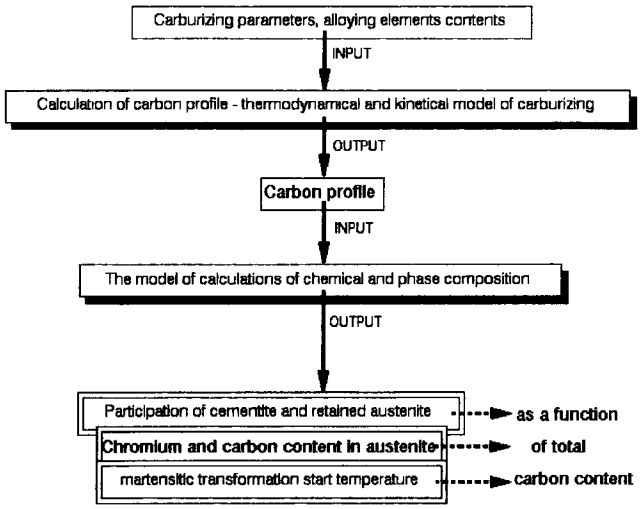

Fig. 30 Diagram of calculation of chemical and phase composition after carburizing

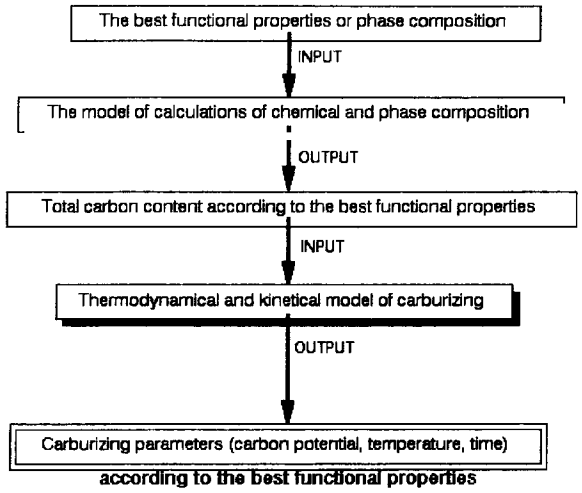

Fig. 31 Diagram of determination of carburizing parameters according to the best functional properties

5. Model Application

Three problems of carburizing of low-chromium hypereutectoid steels were analyzed: (1) thermodynamic and kinetic dependencies at controlled carburizing process in two-phase fields (austenite-cementite); (2) the influence of carbon content on functional properties of carburized low-chromium hypereutectoid steels; and (3) the influence of carbon content on chemical and phase composition of carburized low-chromium hypereutectoid steels.

The models of the calculations are used to: (a) determine chemical and phase composition for carburized layers formed on LH15 (52100) steel at given carburizing parameters; and (b) determine carburizing parameters at assumed chemical and phase composition or functional properties of carburized layer. For (a), the following calculation procedure is applied. Determine carbon profile after carburizing at used carburizing parameters (carbon potential of atmosphere, carburizing time, temperature 1123 K), according to thermodynamic and kinetic model under consideration. (See section 2.) Calculate the chemical and phase composition and the start temperature of martensitic transformation after hardening for given carbon profile, according to equations in section 4. The diagram of this procedure is shown in Fig. 30.

Procedure (b) is performed by the following route. Determine total carbon content, at which the best functional properties are obtained (according to the results presented in section 3) or at which the assumed phase composition is accompanied (section 4). Determine carburizing parameters (carbon potential of the carburizing atmosphere, carburizing time) at which this surface carbon content can be obtained (on the basis of thermodynamic and kinetic model). Figure 31 shows this procedure.

References

1. M. Przylecka, dissertation No. 202 (ISBN 0551-6528), Poznań University of Technology, 1988
2. G. Krauss, *Heat Treatment and Processing Principles,* ASM International, 1990
3. Z. Przylecki, M. Przylecka, M. Kulka, T. Zemcik, J. Suwalski, Z. Kucharski, and M. Lukasiak, *Trait. Thermique,* Vol 264, 1993, p 37-41
4. M. Kulka, M. Przylecka, and W. Gestwa, *Proceedings of the Second ASM Heat Treating and Surface Eng. Conference,* ASM International, 1993, p 87-92
5. M. Kulka, M. Przylecka, W. Gestwa, and W. Budziński, *Proceedings of 9th International Conference,* (Nice, France), PYC Edition, 1994, p 283-290
6. M. Kulka, Ph.D. thesis, Poznań University of Technology, 1993
7. J. Lesage, D. Chicot, M. Przylecka, M. Kulka, and W. Gestwa, *Trait. Thermique,* Vol 276, 1994, p 42-46
8. T. Wada, H. Wada, J.F. Elliott, and J. Chipman, *Metall. Trans.,* Vol 3, 1972, p 1657-1662
9. T. Wada, H. Wada, J.F. Elliott, and J. Chipman, *Metall. Trans.,* Vol 3, 1972, p 2865-2872
10. K. Bungardt, H. Preisendanz, and G. Lehnert, *Arch. Eisenhüttenwes.,* Vol 35, 1964, p 999-1007
11. H. Brandis, H. Preisendanz, and P. Schüler, *Thyssen Edelstahl Tech. Ber.,* Vol 6, 1980, p 155-167
12. K.-H. Sauer, M. Lucas, and H.J. Grabke, *Härt.-Tech. Mitt.,* Vol 43, 1988, p 45-53
13. F. Neumann and B. Person, *Härt.-Tech. Mitt.,* Vol 23, 1968, p 296-308
14. S. Gunnarson, *Härt.-Tech. Mitt.,* Vol 22, 1967, p 293-295
15. S. Ban-ya, J.F. Elliott, and J. Chipman, *Metall. Trans.,* Vol 1, 1970, p 1313
16. M. Przylecka, W. Gestwa, M. Kulka, Carburizing and Carbonitriding Bearing LH15 Steel (52100), *Proceedings of International Heat Treating Conference: Equipment and Processes* (Schaumburg, IL), G.E. Totten and R.A. Wallis, Ed., ASM International, 1994, p 233-238
17. M. Kulka, M. Przylecka, W. Gestwa, and M. Piwecki, *Proceedings of the Second ASM Heat Treating and Surface Eng. Conference* (Dortmund), E.J. Mittemeijer, Ed., Trans. Tech. Publications, 1993, p 215-220
18. M. Przylecka, W. Gestwa, and M. Kulka, *Proceedings of VI Conference Termoobróbka '92,* The Centre of Technical Progress, 1992, p 150-159

19. M. Przylecka, M. Kulka, and W. Gestwa, The Influence of Carbon Content on Functional Properties in Two-Phase Fields, Extended Abstracts Volume, *Proceedings of the 14th International Scientific Conference on Advanced Materials & Technologies* (Gliwice-Zakopane, Poland), L.A. Dobrzanski, Ed., Organizing Committee of International Scientific Conference, 1995, p 369-372; also Carburizing Lengthens Bearing-Element Life, *Advanced Mater. Process.*, Vol 149 (No. 2), 1996, p 52
20. M. Przylecka and A. Perteck, *Proceedings of International Conference—XIVth National Days of Heat Treatment* (Bratislava-Strbske Pleso), The House of the Union Slovak Scientific and Technical Societies, 1992
21. W. Steven and A.G. Haynes, *J. Iron Steel Inst.*, Vol 203, 1965, p 721-727
22. G. Parrish, *Heat Treat. Met.*, Vol 4, 1976, p 102
23. D.P. Koistinen and R.E. Marburger, *Acta Metall.*, Vol 7, 1959, p 59-60
24. R.C. Sharma, G.R. Purdy, and J.S. Kirkaldy, *Metall. Trans. A*, Vol 10, 1979, p 1119-1126